THEORETICAL MODELING OF SPRITES AND JETS

Victor P. Pasko
Communications and Space Sciences Laboratory, Department of Electrical Engineering, The Pennsylvania State University, University Park, PA 16802, USA.

Abstract An overview of the recent modeling efforts directed on interpretation of observed features of transient luminous events (TLEs) termed sprites, blue jets, blue starters and gigantic jets is presented. The primary emphasis is placed on discussion of similarity properties of gas discharges and interpretation and classification of the observed features of TLEs in the context of previous experimental and theoretical studies of gas discharges of various types. Some of the currently unsolved problems in the theory of TLEs are also discussed.

12.1 Introduction

Transient luminous events (TLEs) are large scale optical events occurring at stratospheric and mesospheric/lower ionospheric altitudes, which are directly related to the electrical activity in underlying thunderstorms (e.g., Sentman et al., 1995; Neubert, 2003; Pasko, 2003b) and references cited therein. Although eyewitness reports of TLEs above thunderstorms have been recorded for more than a century, the first image of one was captured only in 1989, serendipitously during a test of a low-light television camera (Franz et al., 1990). Since then, several different types of TLEs above thunderstorms have been documented and classified. These include relatively slow-moving fountains of blue light, known as 'blue jets', which emanate from the top of thunderclouds up to an altitude of 40 km (e.g., Wescott et al., 1995, 2001; Lyons et al., 2003a); 'sprites' that develop at the base of the ionosphere and move rapidly downwards at speeds up to 10,000 km/s (e.g., Sentman et al., 1995; Lyons, 1996; Stanley et al., 1999) and 'elves', which are lightning induced flashes that can spread over 300 km laterally (e.g., Fukunishi et al., 1996a; Inan et al., 1997). Recently several observations of 'gigantic jets', which propagated upwards from thunderclouds to altitudes about 90 km, have been reported (Su et al., 2003). It appears from observations using orbiting sensors that TLEs occur over most regions of the globe (in temperate and tropical areas, over the

M. Füllekrug et al. (eds.), "Sprites, Elves and Intense Lightning Discharges", 253–311.
© 2006 *Springer. Printed in the Netherlands.*

oceans, and over the land) (Boeck et al., 1995; Yair et al., 2003, 2004; Blanc et al., 2004; Israelevich et al., 2004; Su et al., 2004; Mende et al., 2004). To date TLEs have been successfully detected from ground and airborne platforms in North America (e.g., Sentman et al., 1995), Central and South America (e.g., Heavner et al., 1995; Holzworth et al., 2003; Pinto Jr. et al., 2004), in the Caribbean region (Pasko et al., 2002a,b) in Australia (Hardman et al., 1998, 2000), over winter storms in Japan (e.g., Fukunishi et al., 1999; Hobara et al., 2001; Hayakawa et al., 2004), on the Asian continent and over the oceans around Taiwan (e.g., Su et al., 2002, 2003; Hsu et al., 2003) and in Europe (Neubert et al., 2001).

The total electrostatic energy associated with charge separation inside a thundercloud is on the order of 1-10 GJ and a substantial fraction of this energy is released in one lightning discharge on time scales less than 1 sec (e.g., Raizer, 1991, p. 372), making lightning one of the most spectacular and dangerous phenomena on our planet. One of the important aspects of lightning phenomena at low altitudes is that the energy release is happening in highly localized regions of space leading to formation of spark channels with temperatures $\sim$25000°K and plasma with electron densities exceeding $10^{17}\mathrm{cm}^{-3}$ (e.g., Raizer, 1991, p. 373). Due to the exponential decrease in the atmospheric neutral density as a function of altitude even a small fraction of the thundercloud electrostatic energy released at mesospheric/lower ionospheric altitudes during TLE phenomena may have a profound effect on the thermal and chemical balance of these regions; nevertheless these important aspects of TLEs are not yet well understood and quantified. Although the bright ionized channels observed in TLEs (e.g., Gerken and Inan, 2002, 2003, 2005; Pasko et al., 2002a) may indicate high localized energy deposition rates, very little is known at present about actual microphysics of these important elements of TLEs and their effects.

Early theories of TLEs have been reviewed by Rowland (1998), Sukhorukov and Stubbe (1998) and Wescott et al. (1998). The goal of this chapter is to provide a limited overview of some of the recent modeling efforts directed on interpretation of observed features of TLEs termed sprites and jets. We primarily attempt to interpret and classify the observed features in the context of previous experimental and theoretical studies of gas discharges of various types. Some of the currently unsolved problems in theory of TLEs are also discussed.

12.1.1 Phenomenology of Sprites

Sprites are large luminous discharges, which appear in the altitude range of $\sim$40 to 90 km above large thunderstorms typically following intense positive

cloud-to-ground lightning discharges (e.g., Sentman et al., 1995; Boccippio et al., 1995).

The remote sensing of sprite-producing lightning discharges using Extremely-Low Frequency (ELF) waves and by utilizing a known charge moment change threshold for sprite initiation (see Section 12.3.1 for a definition of the charge moment change) provides an estimate of the global occurrence rate of sprites $\sim$720 events/day on average (Sato and Fukunishi, 2003). However, it is known that sprites are not always associated with ELF transients (e.g., Price et al., 2004), and estimates by other authors indicate that 80% of ELF signatures produced by positive lightning are related to sprites (Füllekrug and Reising, 1998), but only 20% of all sprites are associated with ELF signatures (Füllekrug et al., 2001; Reising et al., 1999), which leads to an estimate of $\sim$5 sprite events/minute or 7200 events/day globally (Füllekrug and Constable, 2000).

Recent telescopic imaging of sprites at standard video rates (i.e., with $\sim$16 ms time resolution) revealed an amazing variety of generally vertical fine structure with transverse spatial scales ranging from tens to a few hundreds of meters (Gerken et al., 2000; Gerken and Inan, 2002, 2003, 2005). First high-speed (1 ms) telescopic imaging of sprites has been reported indicating that streamer-like formations in sprites rarely persist for more than 1-2 ms (Marshall and Inan, 2005). Also recently, it has been demonstrated that sprites often exhibit a sharp altitude transition between the upper diffuse and the lower highly structured regions (Stenbaek-Nielsen et al., 2000; Pasko and Stenbaek-Nielsen, 2002; Gerken and Inan, 2002, 2003, 2005). Many sprites are observed with an amorphous diffuse glow at their tops, the so-called sprite "halo" (e.g., Barrington-Leigh et al., 2001; Wescott et al., 2001; Miyasato et al., 2002, 2003; Moudry et al., 2003; Gerken and Inan, 2003; Moore et al., 2003).

In addition to well documented optical and ELF/VLF radiation associated with sprites, well distinguishable infra-sound signatures of these events have recently been reported (Liszka, 2004; Farges et al., 2005).

The appearance of the fine structure in sprites has been interpreted in terms of positive and negative streamer coronas, which are considered as scaled analogs of small scale streamers, and which exist at high atmospheric pressures at ground level (e.g., Pasko et al., 1998a; Raizer et al., 1998; Petrov and Petrova, 1999; Pasko et al., 2001; Pasko and Stenbaek-Nielsen, 2002). These aspects of sprite phenomenology will be discussed in Section 12.3 of this chapter.

12.1.2 Phenomenology of Blue Jets, Blue Starters and Gigantic Jets

Blue jets develop upwards from cloud tops to terminal altitudes of about 40 km at speeds of the order 100 km/s and are characterized by a blue conical

shape (Wescott et al., 1995, 1998, 2001; Lyons et al., 2003a). Blue starters can be distinguished from blue jets by a much lower terminal altitude. They protrude upward from the cloud top (17-18 km) to a maximum altitude of 25.5 km (Wescott et al., 1996, 2001). Blue jets were originally documented during airplane based observations (Wescott et al., 1995). Ground observations of blue jets are believed to be difficult due to severe Rayleigh scattering of blue light during its transmission through the atmosphere (Wescott et al., 1998; Heavner et al., 2000, p. 74). Several ground based video recordings of blue jets, which also electrically connected a thundercloud with the lower ionosphere, have recently been reported (Pasko et al., 2002a; Su et al., 2003; Pasko, 2003b). This type of events is now termed gigantic jets (Su et al., 2003). Recent photographic (Wescott et al., 2001) and video (Pasko et al., 2002a) observations of blue jets at close range have clearly shown the small scale streamer structure of blue jets, earlier predicted in (Petrov and Petrova, 1999), and similar to that reported in sprites. The modeling interpretation of the observed features of blue jets will be presented in Section 12.4.

12.2 Classification of Breakdown Mechanisms in Air

12.2.1 Concept of Electrical Breakdown

The subject of gas discharge physics is very broad and is extensively covered in many textbooks devoted to industrial applications of plasmas and to studies of electrical phenomena associated with naturally occurring lightning (e.g., Raizer, 1991; Roth, 1995, 2001; Lieberman and Lichtenberg, 1994; van Veldhuizen, 2000; Rakov and Uman, 2003; Cooray, 2003; Babich, 2003). In the most general sense, the electrical breakdown is the process of transformation of a non-conducting material into a conductor as a result of applying a sufficiently strong field (Raizer, 1991, p. 128). The specific observed features depend on many factors, including: gas pressure (p), inter-electrode gap size (d), applied electric field (E) magnitude, polarity and time dynamics, electrode geometry, gas composition, electrode material, external circuit resistance, levels of medium pre-ionization, initial energy of seed electrons, etc. (e.g., Raizer, 1991, Chapters 7–12). The presence of electrodes (i.e., the cathode serving as a source of secondary electrons in the discharge volume due to positive ion bombardment) represents an important component of the classical Townsend/Paschen breakdown theory based on simple exponential multiplication of electrons as a function of distance from the cathode, with no significant space charge effects (e.g., Roth, 1995, p. 275). Although the presence of such electrodes, or their analogs, is not immediately obvious in the case of TLE discharges, some of the discharge events (i.e., needle-shaped filaments of ionization, called streamers, embedded in originally cold (near room temperature) air and driven by strong fields due to charge separation in their

heads (Raizer, 1991, p. 334)) can effectively proceed without any significant contribution from the secondary cathode emission. The streamers also serve as precursors to a more complicated leader phenomenon, which involves significant heating and thermal ionization of the ambient gas and which represents a well known initiation mechanism of breakdown in long gaps and in lightning discharges at near ground pressure (Raizer, 1991, p. 363). The understanding of particular parameter regimes in which streamer and leader discharges can occur may therefore still be useful for interpretation of TLE events, even though the electrode dominated Townsend/Paschen theory is not directly applicable to them. In the following subsections we provide a brief overview of a classification of breakdown mechanisms in terms of pd and E/p (or E/N, where N is the ambient gas number density) values. The usefulness of these two parameters will be further discussed in Section 12.2.4 devoted to discussion of similarity properties of gas discharges.

12.2.2 Classification of Breakdown Mechanisms in Terms of pd Values

Here we assume relatively low overvoltage conditions, with overvoltage defined as ΔV=V-V_b, where V_b is the Paschen theory breakdown voltage (e.g., Roth, 1995, p. 278).

At pd values such that pd<10^{-3} Torr·cm an electron crosses the gap practically without collisions, so there is no multiplication of electrons in the discharge volume (Raizer, 1991, p. 137). In this chapter we choose Torr as a unit for pressure (760 Torr = 760 mmHg = 1 atm = 101.3 kPa = 1.013 bar) following commonly accepted practice in existing literature on gas discharges (e.g., Raizer, 1991; Lieberman and Lichtenberg, 1994; Roth, 1995).

The 10^{-1}<pd<200 Torr·cm is the Paschen curve range in which Townsend's breakdown model of multiplication of electron avalanches via secondary cathode emission is predominant (Raizer, 1991, p. 325). This is a parameter regime under which glow discharges typically operate. The glow discharge can be generally defined as a self-sustaining discharge at a moderately large pd (10^{-1}<pd<200 Torr·cm) with a cold cathode emitting electrons due to secondary emission mostly due to positive ion bombardment (Raizer, 1991, p. 167). The discharge is self-sustained in a sense that it can maintain itself in a steady state of primitive reproduction of electrons in the discharge volume, when total outflow of electrons and ions through the boundaries is fully compensated by inflow due to the emission of secondary electrons from the cathode and production of both types of species in the discharge volume due to ionization (Roth, 1995, p. 275). Typical characteristics of stable glow discharges used in practical applications include: tube radius $R\simeq$1 cm, tube length $L\simeq$10-100 cm, pressure $p\simeq10^{-2}$-10 Torr, voltage $V\simeq10^{2}$-10^{3} V and

current $I \simeq 10^{-4}$-10^{-1} A (Raizer, 1991, p. 167; Roth, 1995, p. 284) . The discussion of voltage-current characteristic, distribution of glow intensity and nomenclature of various regions appearing in low pressure DC discharges can be found in numerous textbooks on the subject, some of which are cited at the beginning of the preceding Section 12.2.1. For the purposes of this chapter we only note that the cathode region layered structures observed in low pressure DC discharges generally scale with pressure p as a mean free path of electrons λ_e ($\lambda_e \sim 1/p$) (Raizer, 1991, p. 168). At p=0.1 Torr (65 km altitude) in air $\lambda_e \sim$ 0.3 cm leading to the important conclusion that the dark horizontal bands and bright beads with sizes of tens of meters, which are sometimes observed in sprite discharges (e.g., Gerken and Inan, 2002), cannot be explained by using direct analogy with stratification observed in discharge tubes at the same pressure. It is also well known that the presence of boundaries in discharge tubes, and loss (due to ambipolar diffusion) and production (i.e., due to secondary electron emission) of charged particles on these boundaries play a definitive role in maintaining the particle and energy balance in this type of discharges and in defining the discharge properties (i.e., temperature and density of electrons) (e.g., Lieberman and Lichtenberg, 1994, p. 454). In contrast to discharge tubes in which electron energy distributions are defined by the balance of the ambipolar diffusion of discharge plasma to the walls and production of charged particles in the discharge volume, the energy distributions in large volumes of TLEs are controlled by the local electric field (see discussion and related supporting references concerning the local field approximation in Liu and Pasko, 2004). Additionally, discharge tubes most commonly operate under quasi-steady conditions, which do not directly correspond to sprite discharges having a very transient nature (see Section 12.3.1). The discharge tubes therefore cannot be used as direct analogs of sprite discharges and comparison of any visually similar aspects of these two should be done carefully and with full realization of the above discussed physical differences.

In the range $200 < pd < 4000$ Torr·cm the Townsend and streamer breakdown can be observed depending on specific conditions, i.e., electrode geometry, applied voltage, etc. (Raizer, 1991, pp. 327, 342).

In the range $4000 < pd < \sim 10^5$ Torr·cm the Townsend/Paschen theory fails, streamer breakdown dominates. In this range of pd values the breakdown of plane gaps develops much faster than is predicted by multiplication of avalanches through cathode emission in Townsend/Paschen theory. The breakdown proceeds in this case in a streamer form dominated by space charge effects and at much lower fields than predicted by the Paschen's curve. The secondary cathode emission can be ignored because there is not enough time for ions to cross the gap (Raizer, 1991, p. 326).

The streamer breakdown theory was put forward in the 1930's to explain spark discharges (Loeb and Meek, 1940). The theory was based on the con-

cept of a streamer. Streamers are narrow filamentary plasmas, which are driven by highly nonlinear space charge waves (e.g., Raizer, 1991, p. 327). At ground level, the streamer has a radius of $10^{-1} - 10^{-2}$ cm and propagates with a velocity of $10^5 - 10^7$ m/s. The dynamics of a streamer are mostly controlled by a highly enhanced field region, known as streamer head. A large amount of net space charges exists in the streamer head, which strongly enhances the electric field in the region just ahead of the streamer, while screening the ambient field out of the streamer channel. The peak space charge field can reach a value about 4-7 times of the conventional breakdown threshold field E_k (see definition of E_k in Section 12.2.3). This large space charge field results in a very intense electron impact ionization occurring in the streamer head. This ionization rapidly raises the electron density from an ambient value to the level in the streamer channel, resulting in the extension of the streamer channel to the head region. Therefore, streamers are often referred to as space charge waves. The streamer polarity is defined by a sign of the charge in its head. The positive streamer propagates against the direction of the electron drift and requires ambient seed electrons avalanching toward the streamer head for the spatial advancement (e.g., Dhali and Williams, 1987) The negative streamer is generally able to propagate without the seed electrons since electron avalanches originating from the streamer head propagate in the same direction as the streamer (e.g., Vitello et al., 1994; Rocco et al., 2002). At low atmospheric pressures, at sprite altitudes, streamers may be initiated from single electron avalanches in regions, where the electric field exceeds the conventional breakdown threshold field E_k (see Figure 6 and related discussion in Section 12.3.4). In this case double-headed streamers are expected to form (e.g., Loeb and Meek, 1940; Kunhardt and Tzeng, 1988; Vitello et al., 1993) with the negative head propagating upward toward the ionosphere and the positive downward toward the cloud tops, assuming the positive polarity of a typical cloud-to-ground lightning discharge producing sprites (e.g., Hu et al., 2002).

For many years, the studies of streamers in air at ground pressure have been motivated by their known ability to generate chemically active species, which can be used for treatment of hazardous and toxic pollutants (e.g., Kulikovsky, 1997; van Veldhuizen, 2000), and references cited therein, and in connection with high voltage external insulation problems (e.g., Allen and Ghaffar, 1995). The electrons in the streamer head can gain sufficiently high energy to ionize, dissociate, and excite molecules, and the chemically active excited molecules, radicals and atoms can initiate multiple chemical reactions in the ambient air (Kulikovsky, 1997).

The values $pd{>}{\sim}10^5$ Torr·cm correspond to the leader breakdown mechanism. At ground pressure p=760 Torr the leader mechanism is predominant in gaps $\geq$1 m (Raizer, 1991, p. 363).

The above classification represents a highly condensed and simplified version of that given in (Raizer, 1991), nevertheless, when considered in conjunction with similarity laws (Section 12.2.4), it can provide useful insights into expected breakdown features at low pressures in large TLE volumes ($\geq$1000s of km^3). In particular, streamers propagating in relatively cold (i.e., 300 °K) atmospheric pressure (p=760 Torr) air are known to initiate spark discharges in gaps $d\geq$5-6 cm (Raizer, 1991, p. 327). At a typical sprite altitude of 65 km, p=0.1 Torr and an effective spatial scale needed for development of streamers can be estimated as $d\geq$400 m, which is readily available in this system. In atmospheric pressure air leader mechanism works in gaps with $d\geq$1 meter. At 65 km, p=0.1 Torr, the pd=10^5 Torr·cm gives $d\simeq$10 km, so one generally would expect that spatial scales available at sprite altitudes are also sufficient for development of the leader phenomena. Additionally, recent modeling of neutral gas heating times associated with a streamer-to-leader transition processes for the altitude range corresponding to the transient luminous events indicates a substantial relative (scaled by neutral density as discussed in Section 12.2.4) acceleration of the air heating, when compared to the ground level (Pasko, 2003a). This acceleration is attributed to strong reduction in electron losses due to three-body attachment and electron-ion recombination processes in streamer channels with reduction of air pressure. However, the very transient nature of the electric field at mesospheric altitudes (see Section 12.3.1) may prevent the streamer-to-leader transition since the driving field may not persist long enough to cause significant heating of the neutral gas. From this point of view the streamers are expected to dominate at least in the upper portions of sprites. The exact altitude range in which streamer to leader transition occurs in transient luminous events is not known at present and represents one of yet unsolved problems in current TLE research (see Section 12.5.1).

In addition to the time dynamics of the electric field mentioned in the previous paragraph, the medium pre-ionization (i.e., due to the presence of the lower ionospheric boundary) is of great importance for interpretation of discharge processes in transient luminous events. In particular, following arguments presented above we expect the streamer mechanism to be applicable at $\sim$80 km altitude in sprites. However, a relatively dense lower ionospheric electron population prevents streamers from developing, and even though $pd>$4000 Torr·cm, the ionization proceeds at these altitudes in the form of the simplest volumetric multiplication of electrons initially provided by the lower ionospheric boundary (Pasko et al., 1997, 1998b) (this aspect will be further discussed in Section 12.3.2).

12.2.3 Classification of Breakdown Mechanisms in Terms of Applied Electric Field

The magnitude of the applied electric field has a strong effect on the type of discharge, which is observed in gaps with the same pd values. The increase in electric field leads to streamer formation even in relatively short gaps d<5-6 cm at ground pressure. For instance, (Raizer, 1991, p. 342), indicates that in molecular nitrogen gas at 400 Torr in the gap with size d=3 cm the transition between Townsend mechanism of electron multiplication to streamer discharge occurs at $\simeq 17\%$ overvoltage. Therefore, it is essential to attempt a classification of different discharge mechanisms in terms of applied electric field values.

The most important reference field for gas discharges in air is the conventional breakdown threshold field E_k which is defined by the equality of the ionization and dissociative attachment coefficients (e.g., Raizer, 1991, p. 135). We note that at large values $pd \geq$1000 Torr·cm the breakdown voltage V_b defined by the Paschen curve is almost proportional to pd (or d if p is kept constant) and $E_k \simeq V_b/d$ (Raizer, 1991, p.135; Lieberman and Lichtenberg, 1994, p. 460). The E_k field therefore can be used as an approximate reference field needed for Townsend breakdown at relatively high pd values discussed in the previous subsection. We assume $E_k \simeq$32 kV/ which agrees with typical figures observed in centimeters-wide gaps (Raizer, 1991, p. 135), and also with the ionization and two-body attachment models used recently for streamer modeling in (Liu and Pasko, 2004).

The minimum field required for the propagation of positive streamers in air at ground pressure has been extensively documented experimentally and usually stays close to the value E_{cr}^{+}=4.4 kV/cm (Allen and Ghaffar, 1995), in agreement with recent results of numerical simulations of positive streamers (Babaeva and Naidis, 1997; Morrow and Lowke, 1997). The absolute value of the similar field E_{cr}^{-} for negative streamers is a factor of 2-3 higher (e.g., Raizer, 1991; Babaeva and Naidis, 1997, p. 361). One estimate of this field is E_{cr}^{-}=-12.5 kV/cm (in accordance with Figure 7 of Babaeva and Naidis, 1997). It should be emphasized that the fields E_{cr}^{+} and E_{cr}^{-} are the minimum fields needed for the propagation of individual positive and negative streamers, but not for their initiation (e.g., Petrov and Petrova, 1999). Streamers can be launched by individual electron avalanches in large fields exceeding the conventional breakdown threshold E_k, or by initial sharp points creating localized field enhancements, which is a typical case for point-to-plane discharge geometries (e.g., Raizer et al., 1998). The possibility of simultaneous launching (in opposite directions) of positive and negative streamers from a single midgap electron avalanche is well documented experimentally (e.g., Loeb and Meek, 1940; Raizer, 1991, p. 335) and reproduced in numerical experiments (e.g.,

Vitello et al., 1993). In addition to the E_k, E_{cr}^+ and E_{cr}^- fields discussed above there are several other important reference fields, which can most conveniently be described using a so-called dynamic friction force of electrons in air

$$F = \sum_j N_j \sigma_j(\varepsilon) \delta\varepsilon_j$$

which is shown as a function of electron energy in Figure 1. Here the summation is performed over all inelastic processes characterized by energy dependent cross sections $\sigma_j(\varepsilon)$, with the corresponding energy loss per one collision $\delta\varepsilon_j$. The N_j represents a partial density (in m^{-3}) of target molecules in air corresponding to a particular collision process defined by the cross section σ_j (in plotting F in Figure 1 we assumed partial densities $0.8N_0$ and $0.2N_0$ for N_2 and O_2 molecules, respectively, with N_0=2.68$\times 10^{25}$ m^{-3} being a reference value corresponding to ground pressure). The total of 43 different processes were taken into account in Figure 1 using cross sectional data provided by A. V. Phelps at http://jilawww.colorado.edu/www/research/colldata.html. The electron energy losses due to non-zero energy of secondary electrons emerging from ionizing collisions with N_2 and O_2 molecules are accounted for us-

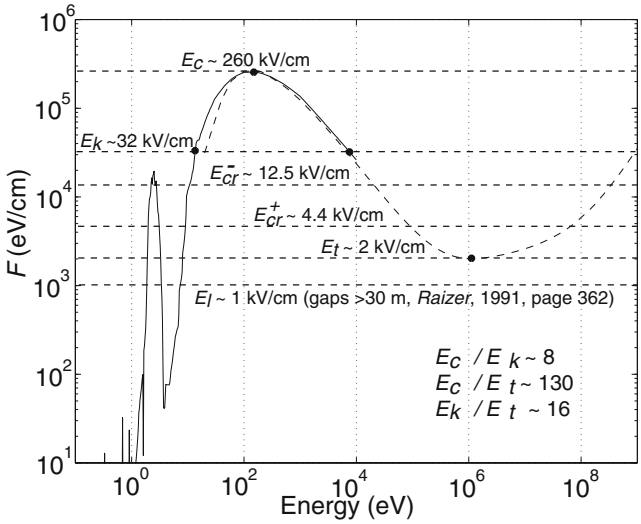

Figure 1. Dynamic friction force of electrons in air. Reference fields (shown by horizontal dashed lines) corresponding to different discharge regimes in air at ground pressure are: E_c – thermal runaway field; E_k – conventional breakdown field; E_{cr}^+ and E_{cr}^- – minimum fields required for propagation of positive and negative streamers, respectively; E_t – relativistic runaway field; and E_l – field needed for advancement of leaders in long gaps (see text for references and discussion).

ing differential ionization cross sections provided in (Opal et al., 1971). The dashed line in Figure 1 shows F values for energy range 20 eV-1 GeV taken from (ICRU, 1984), which combine radiative and collisional losses of electron energy. We note that the radiative losses exceed collisional losses at energy $\sim$100 MeV (ICRU, 1984). The friction force F shown in Figure 1 is conveniently expressed in units of eV/cm and can be directly compared to the applied electric field E in V/cm to provide intuitively simple insight into the expected dynamics of electrons at different energies. We note that F may be directly used in the equation of motion of electrons only under an approximation that electrons move along the applied electric field and scatter mostly in forward direction at small angles (a reasonable approximation above energies $\sim$50 eV). A description for electrons moving at an arbitrary angle with respect to the applied electric field can be found in (Gurevich et al., 1992; Babich, 2003, p. 65). There is a maximum in F at $\sim$150 eV, which is called the thermal runaway threshold ($E_c \simeq$260 kV/cm) and a minimum around $\sim$1 MeV, called the relativistic runaway threshold ($E_t \simeq$2 kV/cm). The maximum is created by a combined action of the ionization and excitation of different electronic states of N_2 and O_2 molecules. At higher energies $>$150 eV the friction force F decreases with increasing electron energy. The main reason for this is that scattering at these energies mostly governed by Coulomb's law interaction of projectile electrons with individual electrons and nuclei constituting ambient gas molecules. The corresponding scattering potential $\sim 1/r$, where r is the center-of-mass scattering radius, leads to scaling of the scattering cross section with energy $\sigma \sim 1/\varepsilon^2$ and effective scaling of $F \sim 1/\varepsilon$ (e.g., Liebermann and Lichtenberg, 1994, p. 57; Gurevich and Zybin, 2001, p. 57). At higher energies the decrease in the dynamic friction force becomes weaker due to relativistic effects; for $\varepsilon \geq$1 MeV it reaches its minimum and then a logarithmically slow increase begins (see Figure 1 in Gurevich and Zybin, 2001). The previously discussed E_k, E_{cr}^+ and E_{cr}^- fields are also shown in Figure 1 by horizontal dashed lines. Additionally, we include a reference minimum field $E_l \simeq$1 kV/cm needed for propagation of leaders in gaps $>$30 m at ground pressure in air (Raizer, 1991, p. 362). It has been shown in the case of lightning discharges that the average field for stable leader propagation can be as low as 100 V/m (Gallimberti et al., 2002, and references cited therein). We note that E_k, E_{cr}^+, E_{cr}^- and E_l fields do not associate with any particular features of the F curve and are shown in Figure 1 simply for easy comparison with E_c and E_t fields.

If we apply to the weakly ionized air an electric field with magnitude above the E_c peak shown in Figure 1, electrons with any (even zero) initial energy will gain more energy from the electric field than they lose in inelastic collisions (i.e., they will become runaway electrons). Some electrons can be energized to very high energies in this way (a substantial population of electrons

will still be present at low energies due to large angle scattering and low energy secondary electrons produced in ionizing collisions). In reality, however, it is not easy to produce and maintain fields above E_c, since the electron runaway is also accompanied by an avalanche multiplication of electrons and strong increase in plasma conductivity, which tends to reduce (screen out) the applied field. At lower fields, comparable to the conventional breakdown threshold field E_k, electrons starting with low energies of several eV are expected to remain at low energies and be trapped in the region of energies $\leq$20 eV, as evident from Figure 1. And finally, at very low applied fields (i.e., a fraction of E_k) electrons are expected to be trapped by the first bump in F around 1-2 eV, which is a result of strong electron energy losses in air due to excitation of vibrational degrees of freedom of nitrogen and oxygen molecules.

As evident from Figure 1, the relativistic threshold field $E_t\sim$2 kV/cm is the minimum field needed to balance the dynamic friction force acting in air on a relativistic electron with $\sim$1 MeV energy (e.g., McCarthy and Parks, 1992; Gurevich et al., 1992; Roussel-Dupré et al., 1994; Lehtinen et al., 1999; Gurevich and Zybin, 2001). In fields above the E_t threshold the 1 MeV electrons, which are readily available in the Earth's atmosphere as cosmic ray secondaries, gain more energy from electric field than they lose in collisions with ambient neutral gas (i.e., become runaways). The possibility of acceleration of energetic cosmic ray secondary electrons in thunderclouds was first suggested by Wilson (1925), and the role of this process in charge redistribution in thunderclouds, in lightning initiation, and in production of observed X-ray fluxes in thunderstorms still remains a subject of active research (see related discussion and references in McCarthy and Parks, 1992; Marshall et al., 1995; Eack et al., 1996b,a; Moore et al., 2001; Dwyer et al., 2003, 2004a,b; Dwyer, 2003, 2004). An interesting aspect of the relativistic runaway process is that an avalanche multiplication of electrons is possible when a fraction of secondary electrons produced in ionizing collisions appear with energies high enough to become runaways themselves (Gurevich et al., 1992; Gurevich and Zybin, 2001). A substantial progress has been made in recent years in modeling of the relativistic runaway process (e.g., Symbalisty et al., 1998; Lehtinen et al., 1999; Gurevich and Zybin, 2001; Dwyer, 2003); and references cited therein. This process has also been extensively discussed in recent literature with applications to TLE phenomena (e.g., Bell et al., 1995; Roussel-Dupré and Gurevich, 1996; Taranenko and Roussel-Dupré, 1996; Lehtinen et al., 1996, 1997, 1999, 2000, 2001; Roussel-Dupré et al., 1998; Yukhimuk et al., 1998a,b, 1999; Kutsyk and Babich, 1999). The relativistic runaway air breakdown is admittedly the most viable mechanism by which terrestrial gamma ray flashes (TGFs) (Fishman et al., 1994; Smith et al., 2005) can be produced in the Earth's atmosphere (Lehtinen et al., 1999, 2001; Inan, 2005; Milikh et al., 2005) and references therein. The first one-to-one correlations of TGF events and light-

ning discharges have been established (Inan et al., 1996; Smith et al., 2005; Cummer et al., 2005; Inan et al., 2005). There is no strong evidence at present time of direct correlation of TGFs and sprites (e.g., Cummer et al., 2005) and the most recent modeling of energy spectrum of TGFs agrees with relativistic runaway breakdown at 16.5 km altitude (Dwyer, 2005).

We note that Figure 1 presents E_k, E_{cr}^+, E_{cr}^-, E_l, E_c and E_t fields at ground pressure. For discussion in this chapter we assume that most of these fields can be directly scaled proportionally to atmospheric pressure p (or neutral density N) to find corresponding values at TLE altitudes. This approach is generally justified by similarity laws for the electric field in gas discharges discussed in the next subsection. We note, however, that the actual scaling of E_{cr}^+ and E_{cr}^- for the altitude range of TLEs has not yet been verified experimentally (see Section 12.5.3), and the simple scaling of E_{cr}^+ and E_{cr}^- proportionally to neutral density adopted in modeling studies discussed in the subsequent sections of this chapter therefore should be considered as one of the approximations, which can be improved as more data on this subject become available. The exact details of the minimum field for leader formation (E_l) scaling with N are not known at present. The E_l field is related to Joule heating processes and may exhibit substantial deviations from the N scaling due to non-similar behavior of this process (see Section 12.2.4).

12.2.4 Similarity Relations

A problem which often arises in the design of DC glow discharge devices is the scaling in size of a glow discharge from a size which is known to work satisfactorily, to a larger or smaller size (Roth, 1995, p. 306). We have already encountered some of the similarity properties of gas discharges earlier in this chapter when we discussed pd values (i.e., discharges preserve similar properties for the same pd=const values) and the scaling of critical breakdown fields proportionally to pressure p (i.e., discharges preserve similar properties for the same E/p=const values). Here we provide a summary of useful similarity relationships for gas discharges. Note that we use neutral density N in place of p therefore assuming constant temperature of ambient neutral gas. The physical quantities with "o" subscript correspond to reference values at ground pressure.

Length (i.e., mean free path, discharge tube length or diameter, streamer radius, etc.) scales as:

$$L = L_o \frac{N_o}{N}$$

(note that this statement can also be written as NL=const, which is identical to the previously discussed pd=const).

Time (i.e., between collisions, dielectric relaxation, 2-body attachment, etc.) scales as:

$$\tau = \tau_o \frac{N_o}{N}$$

Velocity does not scale (i.e., electron or ion drift velocity, streamer velocity, etc.):

$$v = L/\tau = \text{const}$$

Temperature and energy of electrons and ions do not scale remaining the same in similar discharges (for the same reason as v=const).

Electric field (i.e., in streamer head, in streamer body, etc.) scales as:

$$E = E_o \frac{N}{N_o}$$

(note that this statement can also be written as E/N=const, which is identical to the previously discussed E/p=const).

Mobility (electrons and ions) scales as:

$$\mu = v/E = \mu_o \frac{N_o}{N}$$

Diffusion coefficient (electrons and ions) scales as:

$$D = D_o \frac{N_o}{N}$$

Plasma and charge density (i.e., electron and ion densities in the streamer body, etc.) scale as:

$$n = n_o \frac{N^2}{N_o^2}$$

(the above relationship can be easily verified using τ and μ scaling and definition of the dielectric relaxation time $\tau = \varepsilon_o/q_e n\mu$, where ε_o is the permittivity of free space and q_e is the absolute value of electron charge).

Charge (i.e., in the streamer head) scales as:

$$Q = Q_o \frac{N_o}{N}$$

Ionization and two-body attachment coefficients scale as:

$$\nu = 1/\tau = \nu_o \frac{N}{N_o}$$

Conductivity scales as:

$$\sigma = q_e n\mu = \sigma_o \frac{N}{N_o}$$

Current density scales as:

$$J = q_e n v = J_o \frac{N^2}{N_o^2}$$

Current does not scale remaining the same in similar discharges:

$$I = JL^2 = \text{const}$$

The discharge parameters do not always scale in accordance with the above described similarity laws. Examples of processes which do not obey similarity laws are discussed below.

The characteristic time of the three-body attachment of electrons in air (important at high pressures) τ_{a3}=$1/\nu_{a3}$, where ν_{a3} is the three body attachment coefficient, scales as:

$$\tau_{a3} = \tau_{a3o} \frac{N_o^2}{N^2}$$

The joule heating characteristic time scales as

$$\tau_{\rm h} = \tau_{\rm ho} \frac{N_o^2}{N^2}$$

Electron-ion recombination is described by a quadratic term including product of electron and ion densities and therefore does not obey similarity laws (the electron-ion recombination in streamer discharges is dramatically reduced at TLE altitudes due to reduction of electron and ion densities $\sim N^2$ as discussed above).

Non-similarity of photoionization in air is introduced by quenching of N_2 excited states which give rise to UV emissions photoionizing O_2 (e.g., Liu and Pasko, 2004).

Additional discussion of similarity relationships pertinent to a particular case of streamer discharges can be found in (Pasko et al., 1998b).

12.3 Physical Mechanism and Numerical Modeling of Sprites

12.3.1 Large Scale Electrodynamics

The possibility of large-scale gas discharge events above thunderclouds, which we currently know as sprite phenomenon, was first predicted in 1925 by the Nobel Prize winner C. T. R. Wilson (Wilson, 1925). He first recognized that the relation between the thundercloud electric field which decreases with altitude r (Figure 2) as $\sim r^{-3}$ and the critical breakdown field E_k which falls more rapidly (being proportional to the exponentially decreasing atmospheric density) leads to the result that "there will be a height above which the electric

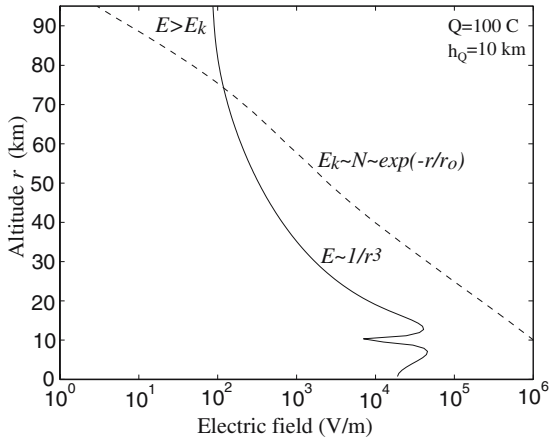

Figure 2. Physical mechanism of sprites Wilson (1925): "While the electric force due to the thundercloud falls off rapidly as r increase, the electric force required to causing sparking (which for a given composition of the air is proportional to its density) falls off still more rapidly. Thus, if the electric moment of a cloud is not too small, there will be a height above which the electric force due to the cloud exceeds the sparking limit."

force due to the cloud exceeds the sparking limit" (Wilson, 1925). It should be noted that due to the finite atmospheric conductivity above thunderclouds the dipole field configuration shown in Figure 2 is realized at mesospheric altitudes only during very transient time periods $\sim$1-10 ms following intense lightning discharges, in part defining similarly transient nature of the observed sprite phenomenon (e.g., Pasko et al., 1997), and references cited therein.

The mechanism of the penetration of the thundercloud electric fields to the higher-altitude regions is illustrated in Figure 3. As the thundercloud charges slowly build up before a lightning discharge, high-altitude regions are shielded from the quasi-electrostatic fields of the thundercloud charges by the space charge induced in the conducting atmosphere at the lower altitudes. The appearance of this shielding charge is a consequence of the finite vertical conductivity gradient of the atmosphere above the thundercloud. When one of the thundercloud charges (e.g., the positive one as shown in Figure 3) is quickly removed by a lightning discharge, the remaining charges of opposite sign above the thundercloud produce a large quasi-electrostatic field that appears at all altitudes above the thundercloud, and endures for a time equal to approximately (see related discussion in Pasko et al., 1997) the local relaxation time ($\tau_\sigma = \varepsilon_o/\sigma$, where σ is the local conductivity and ε_o is the permittivity of free space) at each altitude. These temporarily existing electric fields lead to the heating of ambient electrons and the generation of ionization changes and optical emissions known as sprite phenomena. Figure 4 illustrates the above

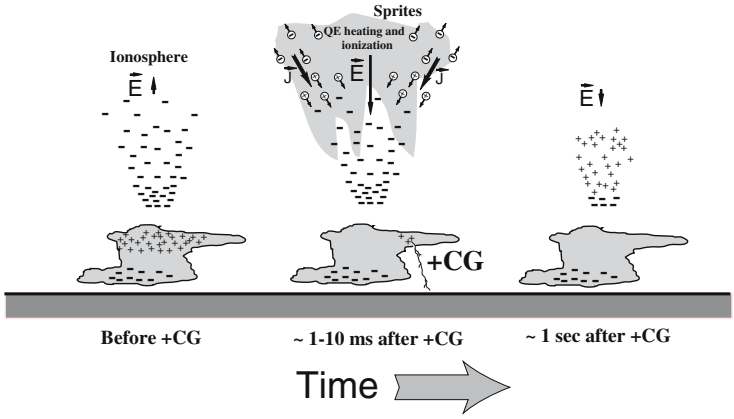

Figure 3. Illustration of the mechanism of penetration of large electric fields to mesospheric altitudes (Pasko et al., 1997). Reprinted by permission from American Geophysical Union.

discussed scenario by showing model calculations of the vertical component of the electric field at altitudes 50, 60, 70 and 80 km directly above a positive lightning discharge removing 200 C of charge from altitude 10 km in 1 ms (Pasko et al., 1997). During a very transient time period $\sim$1 ms, mostly defined by atmospheric conductivity profile, the electric field can reach values on the order of the critical breakdown threshold field E_k at mesospheric/lower ionospheric altitudes. The quasi-static approximation employed here is valid for relatively slow source variations with time scales $>$0.5 ms (Pasko et al., 1999).

It should be emphasized that the simplified schematics shown in Figure 3 is used to discuss the physical concept of penetration of large electric field transients to mesospheric altitudes and by no means reflects the complexity of charge distributions observed in thunderclouds. In cases of more realistic charge distributions in the thundercloud, which sometimes involve up to six charge layers in the vertical direction (e.g., Marshall and Rust, 1993; Shepherd et al., 1996), each of the charge centers can be viewed as generating its own polarization charge in and above the thundercloud, and the resultant configuration of the electric field and charge density can be obtained by using the principle of superposition. This consideration is helpful in visualization of the fact that the electric field appearing at mesospheric altitudes after the charge removal by cloud-to-ground lightning discharge is defined mostly by the absolute value and altitude of the removed charge and is essentially independent of the complexity of the charge configuration in the cloud. The charge removal can also be viewed as the "placement" of an identical charge of opposite sign. The initial field above the cloud is simply the free space field due to the "newly placed" charge and its image in the ground which is assumed to be perfectly conduct-

ing. The most recent observations indicate that most of the charge responsible for production of sprites can be lowered from relatively low altitudes 2-5 km, with an average height 4.1 km for one particular storm studied in (Lyons et al., 2003b), and references therein. The charge moment change Qh_Q (i.e., charge removed by lightning Q times the altitude from which it was removed h_Q) represents the key parameter which is used in current sprite literature to measure the strength of lightning in terms of sprite production potential (e.g., Cummer et al., 1998; Hu et al., 2002; Cummer, 2003). One of the major unsolved problems in current sprite research, which is also directly evident from the Figure 2 depicting the field created by a charge moment Qh_Q=1000 C·km, is the observed initiation of sprites at altitudes 70-80 km by very weak lightning discharges with charge moment changes as small as 120 C·km (e.g., Hu et al., 2002), and references cited therein. Several theories have been advanced to explain these observations, which include localized inhomogeneities created by small conducting particles of meteoric origin (e.g., Zabotin and Wright, 2001) and the formation of upwardly concave ionization regions near the lower ionospheric boundary associated with sprite halos (Barrington-Leigh et al., 2001). The problem of initiation of sprite streamers in low applied electric fields is one of unsolved problems in current TLE research (see Section 12.5.2).

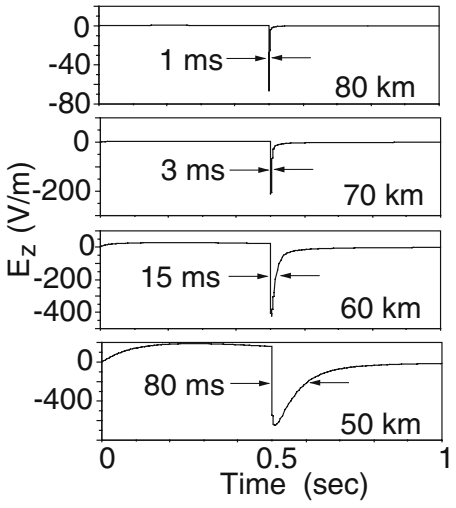

Figure 4. Time dynamics of the vertical component of the electric field at selected altitudes directly above a positive cloud to ground lightning discharge (Pasko et al., 1997). Reprinted by permission from American Geophysical Union.

12.3.2 Altitude Structuring of Optical Emissions

In spite of the apparent simplicity of the basic mechanism of penetration of large quasi-electrostatic fields to the mesospheric altitudes described in the previous section and depicted in Figure 3, the sprite morphology, and sprite altitude structure in particular, appear to be quite complex.

Pasko et al. (1998a) proposed a theory indicating that sprite structure as a function of altitude should exhibit a transition from essentially non-structured diffuse glow at altitudes $\geq$85 km to the highly structured streamer region at altitudes $\leq$75 km (Figure 5). It is proposed that the vertical structuring in sprites is created due to interplay of three physical time scales: (1) The dissociative attachment time scale τ_a (which is defined by the maximum net attachment coefficient as $1/(\nu_a\text{-}\nu_i)_{\max}$, where ν_i and ν_a are the ionization and attachment coefficients, respectively); (2) The ambient dielectric relaxation time scale τ_σ=ε_o/σ; (3) The time scale for the development of an individual electron avalanche into a streamer t_s. This time is an effective time over which the electron avalanche generates a space charge field comparable in magnitude to the externally applied field (e.g., Pasko et al., 1998b). The interplay between these three parameters creates three unique altitude regions as illustrated in Figure 5: (1) The diffuse region ($\tau_\sigma < \tau_a$, $\tau_\sigma < t_s$) characterized by simple volumetric multiplication of electrons (Townsend electron multiplication mechanism); (2) The transition region ($\tau_\sigma > \tau_a$, $\tau_\sigma <\sim t_s$) characterized by strong attachment of ambient electrons before the onset of the electrical breakdown; (3) The streamer region ($\tau_\sigma > \tau_a$, $\tau_\sigma > t_s$) also characterized by the strong attachment as well as by individual electron avalanches evolving into streamers. The upper and the lower boundaries of the transition region shown in Figure 5 represent an estimate of the altitude range in which the actual transition between the diffuse and streamer regions is expected to occur. The upper boundary may shift downward under conditions of an impulsive lightning discharge which generates substantial electron density (i.e., conductivity) enhancement associated with the sprite halo at the initial stage of sprite formation (e.g., Barrington-Leigh et al., 2001). The lower boundary may shift upward due to streamers originating at lower altitudes but propagating upward toward the lower ionosphere (e.g., Stanley et al., 1999). Barrington-Leigh et al. (2001) conducted one-to-one comparison between high-speed video observations of sprites and a fully electromagnetic model of sprite driving fields and optical emissions. Sprite halos are brief descending glows with lateral extent 40-70 km, which are sometimes observed to accompany or precede more structured sprites. The analysis conducted by Barrington-Leigh et al. (2001) demonstrated a very close agreement of model optical emissions and high-speed video observations, and for the first time identified sprite halos as being produced entirely by quasi-electrostatic thundercloud fields. Sprites indeed of-

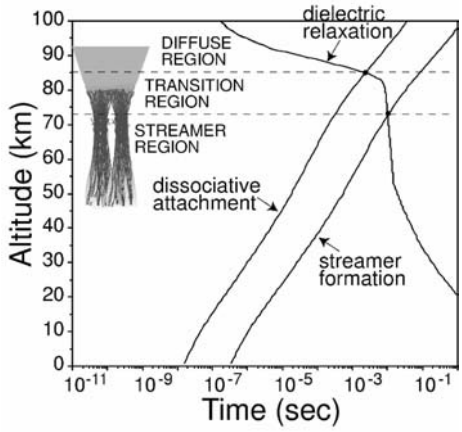

Figure 5. The altitude distribution of different time scales characterizing the vertical structuring of optical emissions in sprites (Pasko et al., 1998b). Reprinted by permission from American Geophysical Union.

ten exhibit sprite halos which appear as relatively amorphous non-structured glow at sprite tops, and which convert to highly structured regions at lower altitudes (e.g., Stanley et al., 1999; Gerken et al., 2000, and cited references therein). This vertical structure in sprites is apparent in recent high-speed video images of Stenbaek-Nielsen et al. (2000) and also was reported during telescopic observations of sprites by Gerken and Inan (2002, 2005).

12.3.3 Large Scale Fractal Models of Sprites

The large scale plasma fluid models based on continuity equations for electrons and ions coupled with either Poisson (Pasko et al., 1997) or the full set of Maxwell's equations (Pasko et al., 1998a; Veronis et al., 1999; Barrington-Leigh et al., 2001) have been successfully used to reproduce some of the observed features of sprites, including their ELF radiation (Cummer et al., 1998) and optical emissions coming from their upper diffuse ("halo") region (Barrington-Leigh et al., 2001). Such direct modeling of the lower, highly structured sprite regions poses insurmountable computational difficulties due to the dramatic differences between the scale of individual ionized channels (i.e., streamers) constituting sprites (on the order of several meters Gerken et al., 2000) and the overall spatial extent of sprites (of order 10 to 100 km). To overcome this difficulty, two-dimensional (Pasko et al., 2000) and three dimensional (Pasko et al., 2001) fractal models have been proposed, which allow the reproduction of the observed large scale volumetric shapes of sprites. One of the important questions, which can be studied with this type of models

is the question about attachment of sprites to cloud tops (Pasko et al., 2001). This question is of fundamental importance for understanding a role of sprites in the global atmospheric electric circuit, since it directly relates to the possibility of establishing a highly conducting link between the Earth's surface and the lower ionosphere. The fractal type of the model simulates the propagation of branching streamers associated with sprites as a growth of fractal trees composed of a large number of line channels, and allows realistic modeling of upward, downward and quasi-horizontal propagation and branching of sprite ionization. The model is based on a phenomenological probabilistic approach, which was proposed in (Niemeyer et al., 1989) for modeling of a streamer corona and uses experimentally and theoretically documented properties of positive and negative streamers in air for a realistic determination of the propagation of multiple breakdown branches in a self-consistent electric field. The fractal model effectively follows the dynamics of highly branched streamers in large volumes of space without actually resolving the internal physics of individual streamer channels, but rather relying on demonstrated collective characteristics of streamers in air (Pasko et al., 2000). The fractal model uses E_{cr}^{+}=4.4 kV/cm and E_{cr}^{-}=12.5 kV/cm as minimum electric field magnitudes required for propagation of positive and negative streamers in air at ground pressure, respectively (see discussion in Section 12.2.3). The critical fields E_{cr}^{+} and E_{cr}^{-} are assumed to scale with altitude proportionally to the atmospheric neutral density as shown in Figure 6.

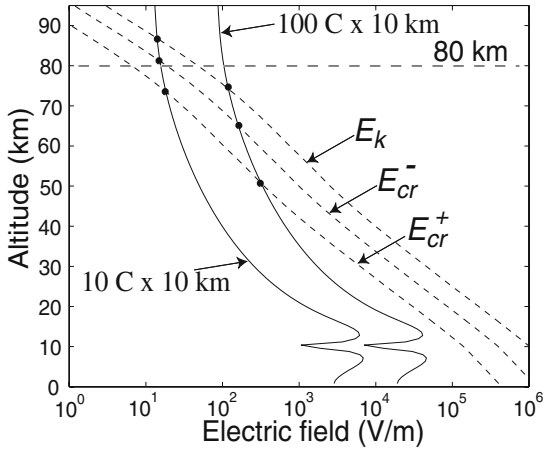

Figure 6. Altitude scans of the electrostatic field corresponding to two different charge moments. The conventional breakdown field E_k, and the minimum fields required for the propagation of positive (E_{cr}^{+}) and negative (E_{cr}^{-}) streamers are also shown for reference by the dashed lines (Pasko et al., 2000). Reprinted by permission from American Geophysical Union.

Figures 7a, 7b and 7c illustrate the development of a sprite initiated by a single electron avalanche at altitude 80 km using a two-dimensional version of the fractal model (Pasko et al., 2000). The starting field is defined by the removal of +100 C of charge by a positive cloud-to-ground (CG) lightning from 10 km altitude (Figure 6). The sprite is characterized by the upward development of negative, and downward development of positive, streamers. This behavior agrees with high speed video observations of initial sprite development (Stanley et al., 1999). We note that this type of model cannot provide information on the velocity of streamers. Figure 7b illustrates the moment of attachment of negative streamers to the lower ionosphere and Figure 7c shows the final configuration after the arresting of propagation of all streamer trees. A large "jelly fish" sprite is formed with its lower extremities reaching an altitude of $\sim$38 km. Figure 7d illustrates the corresponding configuration of the field characterized by the expulsion of the field from the body of the sprite and the enhancement of the field on the sharp edges of streamer trees. As was already emphasized previously the field exceeding the conventional breakdown threshold E_k is needed for initiation of streamers from individual electron avalanches. The initiated streamers can propagate in fields E_{cr}^{+} or E_{cr}^{-}, depending on the streamer polarity, which are substantially lower than E_k. We note that in Figure 7 positive streamers propagated downward well below the point at $\sim$50 km altitude above which the initial field exceeded the E_{cr}^{+} value (Figure 6). This effect is due to self-consistent focusing and enhancement of the field around lower streamer branches (Figure 7d).

12.3.4 Modeling of Small-scale Sprite Streamer Processes and Photoionization Effects

It is well established that the dynamical properties and geometry of both positive and negative streamers can be affected by the population of the ambient seed electrons, and many of the recent modeling studies have been devoted to the understanding of the role of the ambient medium pre-ionization, including effects of photoionization by UV photons originating from a region of high electric field in the streamer head, on the dynamics of negative (e.g., Babaeva and Naidis, 1997; Rocco et al., 2002) and positive (e.g., Babaeva and Naidis, 1997; Kulikovsky, 2000; Pancheshnyi and Starikovskii, 2001) streamers in different mixtures of molecular nitrogen (N_2) and oxygen (O_2) gases, and in air at ground pressure.

The importance of the photoionization effects on sprite streamers at low air pressures at high altitudes is underscored by the fact that the effective quenching altitude of the excited states $b^1\Pi_u$, $b'^1\Sigma_u^+$ and $c_4'^1\Sigma_u^+$ of N_2 that give the photoionizing radiation is about 24 km (corresponding to the air pressure p=p_q=30 Torr) (e.g., Zheleznyak et al., 1982). The quenching of these

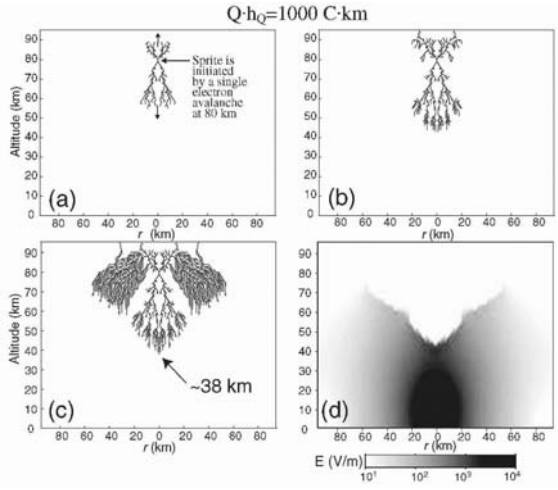

Figure 7. The dynamics of sprite development produced by 100 C of charge removed from 10 km altitude. The sequence of Figures (a)-(c) shows cross-sectional view of discharge trees; (d) A cross-sectional view of the distribution of the absolute values of the electric field corresponding to the structure shown in (c) (Pasko et al., 2000). Reprinted by permission from American Geophysical Union.

states is therefore negligible at typical sprite altitudes 40-90 km, leading to an enhancement of the electron-ion pair production ahead of the streamer tip due to the photoionization, when compared to the previous studies of streamers at ground level. This and other effects have recently been studied by Liu and Pasko (2004) using a newly developed streamer model and some principal results of these studies will be outlined below.

Figure 8 illustrates results of model calculations of electron densities corresponding to double-headed streamers developing at altitudes 0, 30 and 70 km in electric field E_0=1.5E_k. In accordance with the similarity laws (Section 12.2.4), the streamer time scales, the streamer spatial scales, and the streamer electron densities scale with the air density as $\sim 1/N$, $\sim 1/N$, and $\sim N^2$, respectively, and the scaled streamer characteristics remain otherwise identical for the same values of the reduced electric field E/N (Pasko et al., 1998). In order to facilitate discussion of similarity properties of streamers at different altitudes/air densities, the results presented in Figures 8b and 8c are given at the moments of time, which are obtained by scaling ($\sim 1/N$) of the ground value, 2.7 ns, specified in Figure 8a. The horizontal and vertical dimensions of the simulation boxes in Figures 8b and 8c also directly correspond to scaled ($\sim 1/N$) ground values shown in Figure 8a. The electron density scale in Figures 8b and 8c also corresponds to scaled ($\sim N^2$) values given in Figure 8a. The dif-

ferences observed between model streamers at the ground and at 30 and 70 km altitudes in Figure 8 are primarily due to the reduction in photoelectron production at high atmospheric pressures through the quenching of UV emitting excited states of N_2 (Liu and Pasko, 2004). In all cases shown, the model streamers exhibit fast acceleration and expansion (Liu and Pasko, 2004). The results presented in Figure 8 correspond to a "free" (i.e., not affected by electrodes) development of double headed streamers under conditions of the same E/N reduced field values. In this context we note that discussion of similarity of streamers obtained in point-to-plane discharge geometry (e.g., Pancheshnyi et al., 2005; Briels et al., 2005) necessitates inclusion of electrode effects, and, assuming a relatively fast voltage rise time, similar streamer patterns are expected at the same E/N values (see additional discussion of the quenching effects on streamer similarity properties and branching at high pressures in Section 12.5.4) only under conditions when electrode geometry (i.e. inter-electrode distance, point electrode diameter, etc.) are scaled as $\sim 1/N$. The fast expansion and acceleration are important characteristics of the considered model streamers. For instance, a positive streamer initiated in a $1.1E_k$ field at 70 km altitude would reach an effective radius of 55 m and speed of about one tenth of the speed of light (2.2×10^7 m/s) by traveling a distance of only 1 km (Liu and Pasko, 2004). Such high speeds of sprite streamers indeed have

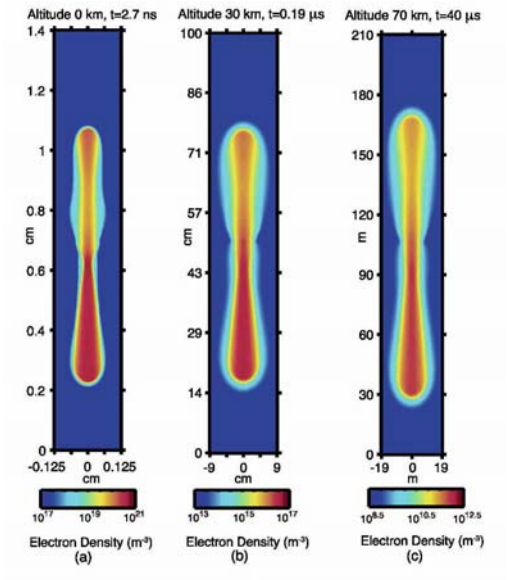

Figure 8. A cross-sectional view of the distribution of the electron number density of the model streamers at altitudes (a) 0 km, (b) 30 km, and (c) 70 km (Liu and Pasko, 2004). Reprinted by permission from American Geophysical Union.

been recently documented by high-speed video (Stanley et al., 1999; Moudry et al., 2002, 2003) and multi-channel photometric (McHarg et al., 2002) systems. The initiation of sprites at altitudes 70-75 km in a form of simultaneous upward and downward propagating streamers is also well documented (Stanley et al., 1999; Stenbaek-Nielsen et al., 2000; Moudry et al., 2002, 2003; McHarg et al., 2002). It is clear, however, that the effective streamer diameters observed by an imager zooming on sprite structures at different altitudes would inevitably depend on the geometry of the mesospheric electric fields and the history of the sprite development (i.e., the altitude of the initiation point(s)). Gerken et al. (2000) and Gerken and Inan (2002, 2003) have recently employed a novel telescoping imager to measure effective streamer diameters at different altitudes in sprites. The measured diameters are 60-145 m ($\pm$12 m), 150 m ($\pm$13 m), 19 m ($\pm$13 m), for altitude ranges 60-64 km ($\pm$4.5 km), 76-80 km ($\pm$5 km), 81-85 km ($\pm$6 km), respectively. Although the 60-145 m ($\pm$12 m) is more than one order of magnitude greater than the scaled initial diameters of streamers shown in Figure 8c (at 60 km, $2r_s \simeq$4 m), given realistic charge moments available for the sprite initiation (Hu et al., 2002), it is likely that streamers appearing at these low altitudes were initiated at much higher altitudes and propagated long distances experiencing substantial expansion. All observed diameters by Gerken et al. (2000) and Gerken and Inan (2002, 2003) can therefore be realistically accounted for by the modeling studies presented in (Liu and Pasko, 2004).

12.3.5 Optical Emissions Associated with Sprite Streamers

Figures 9 and 10 illustrate distributions of the electric field magnitude and intensities of optical emissions (in Rayleighs) corresponding to the model streamers at 30 and 70 km altitudes, respectively, at the same instants of time as specified in Figure 8. The strong blue emissions (associated with 1st negative N_2^+ ($1NN_2^+$) and 2nd positive N_2 ($2PN_2$) band systems, Figures 10c and 10d) originating primarily in the streamer heads are expected to be produced during the early time of sprite development, as the sprite develops over its altitude extent on a time scale short with respect to the total sprite emission time. This agrees well with recent narrow-band photometric and blue-light video observations of sprites (Armstrong et al., 1998, 2000; Suszcynsky et al., 1998; Morrill et al., 2002) indicating short duration ($\sim$ms) bursts of blue optical emissions appearing at the initial stage of sprite formation. The time averaged optical emissions are expected to be dominated by red emissions associated with the first positive band system of N_2 ($1PN_2$, Figure 10b), which has the lowest energy excitation threshold ($\sim$7.35 eV) and can effectively be produced by relatively low electric fields in the streamer channels, in agreement with sprite

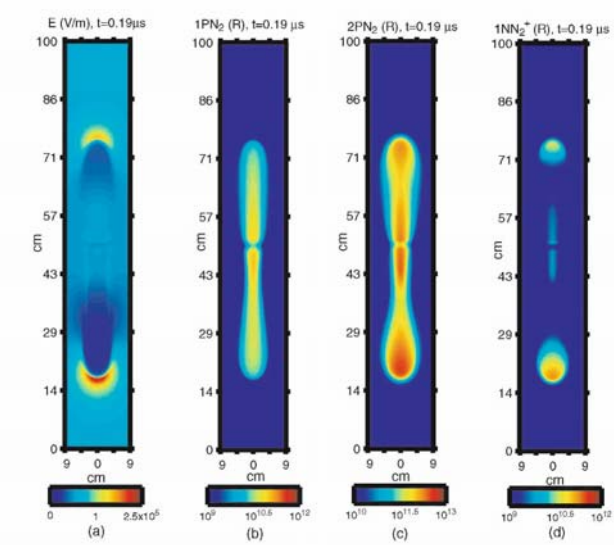

Figure 9. The magnitude of the electric field (a) and the intensity of optical emissions (in Rayleighs) in selected band systems (b)- associated with the model streamers at altitude 30 km (Liu and Pasko, 2004). Reprinted by permission from American Geophysical Union.

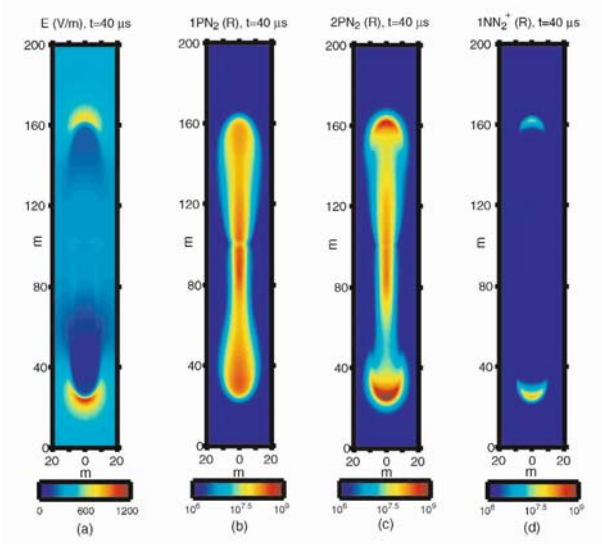

Figure 10. The same as Figure 9 only for model streamers at altitude 70 km (Liu and Pasko, 2004). Reprinted by permission from American Geophysical Union.

observations (Mende et al., 1995; Hampton et al., 1996; Morrill et al., 1998, 2002; Takahashi et al., 2000; Bucsela et al., 2003). We also note that the suppression of $1PN_2$ emissions due to the strong quenching of the $B^3\Pi_g$ state at altitudes below 50 km (e.g., Vallance-Jones, 1974, p. 119) (note the intensity scale difference between Figures 9b and 9c) is the primary factor which is responsible for making the blue color a dominant color of streamer coronas at lower extremities of sprites (e.g., Sentman et al., 1995) and in blue jet type phenomena observed near thundercloud tops (e.g., Wescott et al., 1995). The red ($1PN_2$) emissions are not completely quenched at altitudes $<$50 km and have been detected in red-filtered images of sprites (Armstrong et al., 1998). A detailed calculation of the streamer color requires knowledge of the spectral range of the color TV system, the specifics of the observational geometry, allowing to account for the effects of the atmospheric transmission, and such factors as the transmission through an aircraft window (e.g., Wescott et al., 1998; Morrill et al., 1998). The interested readers can find more discussion on related topics in Section 12.4.2 of (Pasko and George, 2002) and references cited therein. The related aspects will also be discussed with relation to blue jets in Section 12.4.4.

Recently, the ISUAL instrument on FORMOSAT-2 (former ROCSAT-2) satellite has successfully observed far-UV emissions from sprites due to N_2 Lyman-Birge-Hopfield (LBH) band system (Mende et al., 2004; Frey et al., 2004). Modeling results on LBH emissions from sprite streamers at 70 km altitude indicate that the LBH emissions are stronger by up to a factor of 10 than those from the first negative band system of N_2^+ (Liu and Pasko, 2005).

12.4 Physical Mechanism and Numerical Modeling of Blue Jets, Blue Starters and Gigantic Jets

Petrov and Petrova (1999) were first to propose that blue jets correspond qualitatively to the development of the streamer zone of a positive leader and therefore should be filled with a branching structure of streamer channels. These predictions appear to be in remarkable agreement with recent experimental discoveries indicating the streamer structure of blue jets (Wescott et al., 2001; Pasko et al., 2002a). Following the suggestion of Petrov and Petrova (1999), we outline below a possible scenario of events leading to the upward launch of blue jets and blue starters, which occupy large volumes of the atmosphere above thunderstorms measured of thousands of cubic kilometers; many orders of magnitude greater than volumes typically associated with the conventional lightning processes at lower altitudes.

12.4.1 Blue Jets as Streamer Coronas

It is now well-established that electric fields measured from balloons at different altitudes in thunderstorms very rarely exceed 0.5-1 kV/cm (e.g., Winn et al., 1974; Marshall et al., 1996, 2001), and references therein. Results of one study specifically devoted to the investigation of electric field magnitudes and lightning initiation conditions in thunderstorms indicate that in most observed cases the thundercloud electric field as a function of altitude is bounded by the relativistic runaway threshold field E_t, which has a value close to 2 kV/cm at ground level (see Figure 1) and is reduced with altitude proportionally to the atmospheric neutral density (e.g., Marshall et al., 1995). The E_t field has been discussed earlier in Section 12.2.3 and is referred to as the breakeven field in some publications (e.g., Marshall et al., 1995). For the purposes of our discussion in this section we use E_t only as a reference upper bound on fields which are typically observed inside thunderclouds, making no direct association of the relativistic runaway phenomena with blue jets and blue starters. The E_t field as a function of altitude is illustrated in Figure 11. We note that the threshold field E_t appears to be very close to the documented minimum fields ($E_l \sim$1 kV/cm, see Figure 1) required for propagation of positive and negative leaders in long gaps with sizes exceeding several tens of meters at ground pressure (Raizer, 1991, p. 362). The leader process is also a well-documented means by which conventional lightning develops in thunderstorms (Uman, 2001, p. 82). We note that the electric fields in thunderstorms

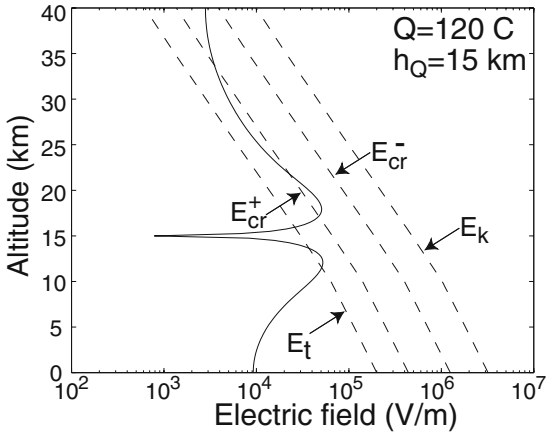

Figure 11. Altitude scan of the electrostatic field produced by a 120 C thundercloud charge placed in the center of the simulation box at altitude 15 km (solid line). Dashed lines show the characteristic fields E_t, E_{cr}^+, E_{cr}^-, and E_k (Pasko and George, 2002). Reprinted by permission from American Geophysical Union.

can occasionally exceed the E_t threshold, and in those rarely observed cases lightning usually followed, immediately destroying the electric field meters at the place where the electric field went substantially above the E_t value (Marshall et al., 1995). In two out of three such cases reported in (Marshall et al., 1995), the E_t threshold was exceeded at altitudes close to 10 km, and in both cases the electric field was upward directed, so that positive streamers would have propagated upward (Marshall et al., 1995). The maximum field enhancement observed by (Marshall et al., 1995) before the instrument was struck and destroyed by lightning is $1.6E_t$. The maximum electric field of 1.86 kV/cm at 5.77 km altitude (i.e., $\sim 1.8E_t$) in close proximity to a lightning initiation location has recently been reported in (Marshall et al., 2005). Another report of electric field observations substantially greater than E_t is that by (Winn et al., 1974), whose authors observed fields on the order of $4E_t$. A summary of other observations of maximum electric field magnitudes measured in thunderclouds is given in (Rakov and Uman, 2003, p. 83). The fact that fields greater than E_t are observed only rarely in balloon sounding data does not necessarily mean that they are uncommon in thunderclouds, if one considers a reasonable argument that regions exhibiting these fields may be localized and also that their persistence in time may be limited by the fast development of a lightning discharge which would try to reduce them. (Marshall et al., 1995) point out that the balloon soundings give the electric field only at the balloon location and that electric fields substantially larger than E_t might be present elsewhere in the cloud.

It is assumed that as soon as the electric field inside the thundercloud approaches the E_t threshold the leader process is developed. The normal role of the leader process is to initiate a discharge of the system, leading to a reduction of charge accumulation in the thundercloud responsible for the field enhancement. The leader process itself is known to be quite complex, and its initiation mechanism and internal physics are not yet fully understood (e.g., Uman, 2001, p. 79; Raizer, 1991, p. 370, Bazelyan and Raizer, 1998, p. 203, 253). For the purposes of discussion here, we do not consider specifics of the leader initiation and postulate presence of this process in high field ($\sim E_t$) regions of the thundercloud.

The head of the highly ionized and conducting leader channel is normally preceded by a streamer zone looking as a diverging column of diffuse glow and filled with highly branched streamer coronas (e.g., Bazelyan and Raizer, 1998, p. 203, 253). Due to its high conductivity, the leader channel can be considered as equipotential and therefore plays the primary role in focusing/enhancement of the electric field in the streamer zone, where the relatively weakly conducting streamer coronas propagate (e.g., Raizer, 1991, p. 364). Leaders of positive polarity attract electron avalanches, while in those of negative polarity the avalanching electrons move in the same direction as the leader head. In large

experimental gaps (>100 m) and in thunderclouds, the electric fields required for propagation of leaders of the positive and negative polarity are known to be nearly identical, but the internal structure of their streamer zones, which is closely associated with the direction of electron avalanches, is very different (Raizer, 1991, p. 375; Bazelyan and Raizer, 1998, p. 253) . We note that the experimentally documented electric fields E_{cr}^{+} and E_{cr}^{-} required for propagation of streamer coronas, which constitute essential components of the leader streamer zone, are substantially higher than the ambient E_t (Figure 1), and as a result the leader streamer zone is normally confined to a limited region of space around the leader head. A remarkable feature of the streamer corona is that in spite of its internal structural complexity, involving multiple highly branched streamer channels, its macroscopic characteristics remain relatively stable under a variety of external conditions and the field measurements inside the streamer zone of positive (Petrov et al., 1994) and negative (Petrov and Petrova, 1993) leaders indicate that the minimum fields required for propagation of positive E_{cr}^{+} and negative E_{cr}^{-} streamers discussed in Section 12.2.3 and shown in Figure 1 are also close to the integral fields established by positive and negative coronas, respectively, in regions of space through which they propagate.

Figure 11 shows an altitude scan of the electric field created by a static charge of 120 C, having a Gaussian spatial distribution with spatial scale 3 km placed at 15 km altitude between two perfectly conducting planes positioned at the ground (0 km) and at 40 km altitude, as well as the critical fields E_t, E_{cr}^{+}, E_{cr}^{-}, and E_k, which assumed to scale with altitude proportionally to the neutral atmospheric density (see additional discussion on scaling in Section 12.5.3 and additional references for physical factors defining the position of the upper boundary at the end of Section 12.4.2).

We note that the fields (E_{cr}^{+}, E_{cr}^{-}, E_k) can be comfortably exceeded at high altitudes (>70 km) following intense positive cloud-to-ground lightning discharges leading to the sprite phenomenon (see Figure 6). However, these fields (especially E_k) are much greater than the large scale fields typically observed inside thunderclouds, as discussed above and illustrated by the E_t altitude distribution shown in Figure 11. The large-scale electric field enhancement inside thunderclouds above even E_{cr}^{+} (which is closest to the E_t) should be considered as an unusual and rare circumstance.

In view of the above discussion it is clear that if, due to the fast growth of the thundercloud charge, the large-scale electric field does exceed the E_{cr}^{+} threshold, then positive streamer coronas, which are normally confined close to the leader head, can quickly (with propagation speeds $>10^5$ m/s, substantially exceeding typical leader speeds $\sim 2\times 10^4$ m/s (e.g., Bazelyan and Raizer, 1998, p. 227) fill a large volume of space in the vicinity of a thundercloud. Such field distribution, which exceeds E_{cr}^{+} in a relatively narrow ($\pm$2 km) re-

gion around 20 km altitude, is illustrated in Figure 11. Although the initial volume of space occupied by streamer coronas is defined by the geometry of thundercloud charges (the volume of space in which electric fields exceed the E_{cr}^{+} threshold), the streamer coronas themselves self-consistently modify the electric field distribution. Results of three-dimensional modeling of streamer coronas under these circumstances (Pasko and George, 2002) clearly demonstrate that under a variety of initial conditions the streamer coronas form upward propagating conical shapes closely resembling the experimentally observed geometry of blue jets. An example of these calculations will be shown in Section 12.4.3 below.

12.4.2 Thundercloud Charge and Current Systems Supporting Blue Jets, Blue Starters and Gigantic Jets

The formulation of large-scale charge and current systems in thunderclouds, which support upward propagation of blue jets and blue starters and which we discuss here, closely follows that given in (Pasko and George, 2002), and is based on a fast-growing positive charge at the thundercloud top. It is assumed that this charge is a primary source of the electric field which drives blue jets and starters, with no association with lightning activity. The positive (top) and the negative (bottom) thundercloud charges (Figure 12) accumulate due to the current $\vec{J}_s'$ associated with the separation of charges inside the cloud and directed opposite to the resulting electric field. We assume that the charge accumulation time scale can in some cases be very fast (fraction of a

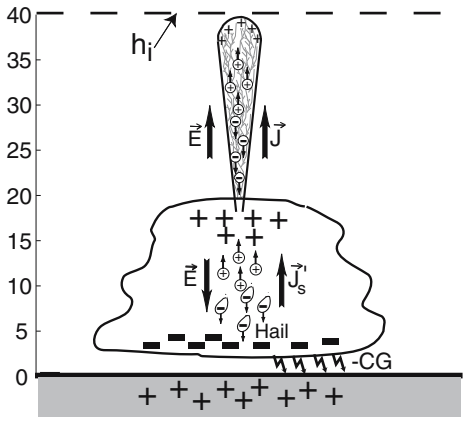

Figure 12. Currents, charges and electric fields associated with blue jets (Pasko and George, 2002). Reprinted by permission from American Geophysical Union.

second). This time scale, in combination with the middle atmospheric conductivity profile, plays a primary role in defining the upper termination altitude of blue jets (Pasko and George, 2002, Section 2.6). The current $\vec{J}_s'$ may be related to the small, light and positively charged ice splinters driven by updrafts and heavy negatively charged hail particles driven downward by gravity (e.g., Uman, 2001, p. 65). Unusually intense precipitation of large hail was indeed observed in association with blue jets and blue starters (Wescott et al., 1995, 1996) and due to negative charge associated with hail particles discussed above is a strong indication of intense electrical activity inside the cloud. The recently observed blue jet event in Puerto Rico (Pasko et al., 2002a) was produced during a fast growth stage of thunderstorm development. The electromagnetic data which was available for both the Wescott et al. (1995, 1996) and the Pasko et al. (2002a) observations indicate no direct triggering of blue jets and blue starters by a lightning event. It is assumed that a charge of $\sim$110-150 C with Gaussian spatial distribution of scale $\sim$3 km can accumulate at altitude $\sim$15 km, creating electric field magnitudes capable of crossing the E_{cr}^{+} threshold as depicted in Figure 11 and discussed in the previous section. As a general note, we emphasize that although our model results presented in the following section depend on the spatial scale of the charge, the charge value and the charge altitude, and these parameters are expected to vary for conditions existing in real thunderclouds, the results appear to be very robust in terms of production of upward conical shapes of blue jets as long as the large-scale fields exceed the E_{cr}^{+} threshold at the thundercloud top. In part this has to do with the general geometry of electric field lines created by a localized charge placed between two conducting plane boundaries and the exponential reduction of E_{cr}^{+} as a function of altitude. Following (Pasko and George, 2002), we neglect the lower (negative) thundercloud charge due to its proximity to the ground (Figure 12). This charge also may be removed by a series of negative lightning discharges during several seconds before the appearance of jets (Wescott et al., 1995, 1996). The electric field is non-zero inside the positive streamer coronas constituting blue jets and blue starters, and an integral upward directed current always flows in the body of the jet (Figure 12). The blue jet propagates when this current is supported by a source in or near the cloud. Otherwise, the negative charge flowing towards the positive thundercloud charge would reduce the source charge and the electric field above the cloud and would eventually suppress the propagation. Thus, the blue jet or blue starter can propagate as long as $\vec{J}_s'$ can deliver sufficient positive charge to the thundercloud top. An equal amount of negative charge is accumulated at the thundercloud base so that the overall charge in the cloud-jet/starter system is conserved. For the fractal model calculations which we show in the next section, we simply assume that the source thundercloud charge remains unchanged during the development of the phenomena, which physically corresponds to a situation when thundercloud current $\vec{J}_s'$ compen-

sates any reduction in the source charge due to the jet current. We note that in the fractal model of Pasko and George (2002) the upper terminal altitude of blue jets is defined by the location of the upper boundary of the simulation box, as discussed in the next section (i.e., 40 km, in Figure 11). The discussion of physical factors, which determine terminal altitudes of blue jets, blue starters and gigantic jets, providing effective classification of different phenomena as a function of their vertical extent, can be found in (Pasko and George, 2002, Sections 2.6 and 4.1).

12.4.3 Numerical Simulation of Blue Jets and Blue Starters

The large scale volumetric shapes of blue jets, blue starters and gigantic jets can be successfully modeled with two and three dimensional fractal models discussed in Section 12.3.3, and related results are documented in (Pasko and George, 2002). Figure 13a shows an example of the model calculation corresponding to the same charge configuration as in Figure 11, but with the upper simulation box boundary set to 70 km altitude, corresponding to the terminal altitude of the blue jet event reported in (Pasko et al., 2002a). Figure 13b shows one of the images of the blue jet phenomena, taken from the video sequence reported in (Pasko et al., 2002a) and corresponding to the moment of the attachment of the blue jet to the lower ionospheric boundary. This stage of the blue jet development is similar to the "final jump stage" of the leader process observed in laboratory experiments, when the streamer zone makes contact with the opposite electrode (Bazelyan and Raizer, 1998, p. 212). The range of observed speeds during the final jump, 5×10^4 m/s to 10^6 m/s (Bazelyan and

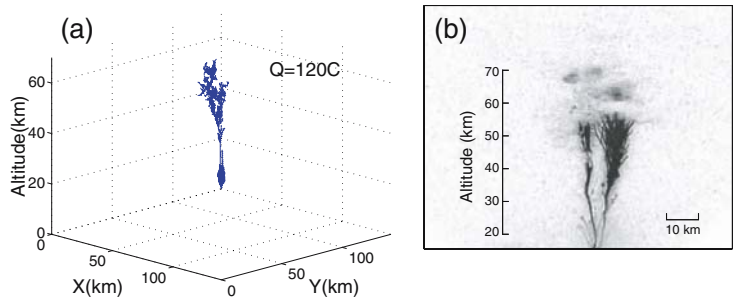

Figure 13. (a) Fractal model results for thundercloud charge Q=120 C at altitude h_Q=15 km and the upper simulation box boundary at 70 km (Pasko and George, 2002). Reprinted by permission from American Geophysical Union. (b) Image of a blue jet at the moment of attachment to the lower ionospheric boundary (Pasko et al., 2002a). Reprinted by permission from *Nature*.

Raizer, 1998, p. 212), is similar to the range of speeds, from 5×10^4 m/s to more than 2×10^6 m/s, reported in (Pasko et al., 2002a). Although this type of model cannot provide information on the velocity of streamer coronas, Figure 13 demonstrates a good agreement between model results and observations in terms of the general volumetric shape of the blue jet.

12.4.4 Modeling of Optical Emissions from Blue Jets and Blue Starters

Blue jets and blue starters have been captured by black and white and color video cameras, allowing for some important suggestions concerning optical bands responsible for the observed blue color (Wescott et al., 1995). Evidence from color TV suggesting that the blue light must have an ionized 1st negative N_2^+ component has been presented in (Wescott et al., 1998). The first conclusive evidence of 427.8 nm (1st negative N_2^+) emission in blue starters has been recently reported in (Wescott et al., 2001). Wescott et al. (2001) also analyzed color TV frames associated with blue starters and concluded that the combined red and green channel intensity constituted 7% of the total blue channel intensity.

The fractal model allows accurate determination of the macroscopic electric fields in regions of space occupied by streamers. The results reported in (Pasko and George, 2002) indicate that for a variety of input parameters these fields are very close (within several %) to the minimum electric field required for propagation of positive streamers in air, E_{cr}^+. This behavior is consistent with earlier findings (Niemeyer et al., 1989; Pasko et al., 2000, 2001) and experimental measurements of Petrov et al. (1994). We note, however, that the low fields on the order of E_{cr}^+ are generally not sufficient to excite any observable optical emissions (Pasko and George, 2002).

The fractal model does not allow resolution of microscopic properties of individual streamer channels constituting streamer coronas and therefore does not allow resolution of the regions of space around streamer tips. It is known that under a variety of conditions the electric field enhancements around streamer tips reach values $\sim 5E_k$ (e.g., Dhali and Williams, 1987; Vitello et al., 1994; Babaeva and Naidis, 1997; Kulikovsky, 1997; Pasko et al., 1998b), where E_k is the conventional breakdown threshold field discussed in Section 12.2.3 and shown in Figure 1. This property of streamers is also valid for positive streamers propagating in low ambient electric fields comparable to E_{cr}^+ (e.g., Grange et al., 1995; Morrow and Lowke, 1997), similar to the ambient conditions for propagation of streamer coronas considered in (Pasko and George, 2002) and illustrated in the previous section. Our conclusion, therefore, is that the observed optical luminosity in blue jets and starters arises from

large electric fields existing in narrow regions of space around tips of small-scale corona streamers constituting them.

Figure 14 presents comparison of recent spectral observations reported by Wescott et al. (2001) and the calculated ratio of the combined red and green emissions to the total blue emission assuming the driving field to be $5E_k$, using optical model formulation documented in (Pasko and George, 2002; Liu and Pasko, 2004), and also accounting for the atmospheric transmission and aircraft window corrections pertinent to experimental conditions of (Wescott et al., 2001). The resultant ratio appears to be in good agreement with the recent analysis of color TV frames associated with blue starters reported in (Wescott et al., 2001), who concluded that the combined red and green channel intensity constituted 7% of the total blue channel intensity.

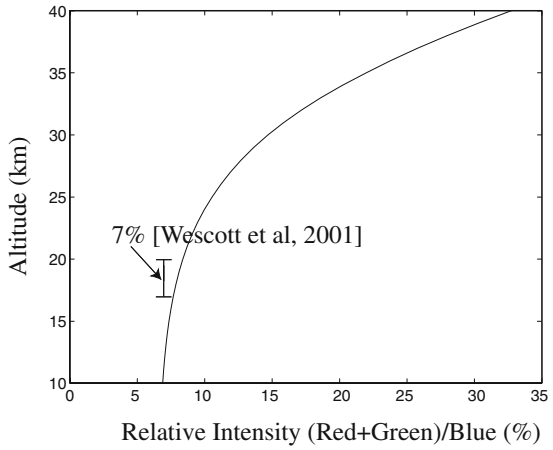

Figure 14. Ratio of the combined red and green emissions to the total blue emission as a function of altitude (Pasko and George, 2002). Reprinted by permission from American Geophysical Union.

12.5 Unsolved Problems

12.5.1 Relationship of Sprites and Jets to High Air Pressure Leader Processes

Although the streamer-to-leader transition (e.g., Raizer, 1991, p. 363); (Bazelyan and Raizer, 1998, p. 238), may be a part of the blue jet/starter and even sprite phenomena, their branched appearance is suggestive that their initial formation is due mostly to the streamer coronas expanding from the leader streamer zone at lower altitudes in case of blue jets, and from single electron avalanches, or some other, yet unknown, initiation agents in case of sprites.

The available imaging data reported recently in Wescott et al. (2001); Pasko et al. (2002a); Su et al. (2003), and some earlier observations of lightning-like phenomena at thundercloud tops reviewed recently in (Lyons et al., 2003a) indicate that the streamer-to-leader transition may be occurring in the lower parts of blue jets and at the later stages of their development (see also related discussion in Pasko and George, 2002). The transition involves a collective action of streamers leading to an increase in ambient gas temperature to several 1000s of °K sufficient for development of the thermal ionization (Raizer, 1991, p. 365). In this respect we note that the understanding of ambient gas heating processes initiated by streamers, embedded in originally cold (near room temperature) air represent a long standing problem, which is of interest for studies of long laboratory sparks and natural lightning discharges (e.g., Gallimberti et al., 2002). As we have already discussed in Section 12.3.4, many of the small-scale features observed in sprites at higher altitudes (e.g., Gerken and Inan, 2003) can be interpreted in terms of corona streamers, which, after appropriate scaling with air density, are fully analogous to those, which initiate spark discharges in relatively short (several cm) gaps at near ground pressure (Liu and Pasko, 2004, and references therein), and which constitute building blocks of streamer zones of conventional lightning leaders in long gaps (Gallimberti et al., 2002). The recent reports of infrasound bursts originating from 60-80 km altitudes in sprites, with durations consistent with the optical widths of the sprites (Farges et al., 2005), and recent modeling results indicating the relative acceleration of the air heating with reduction of pressure discussed in Section 12.2.2, provide additional motivation for studies of the heating of the ambient air and associated chemical effects caused by streamers in transient luminous events. The streamer-to-leader transition at low air pressures represents one of unsolved problems in current TLE research.

12.5.2 Initiation of Sprite Streamers in Low Applied Fields

As it has already been briefly mentioned in Section 12.3.1, the initiation mechanisms of sprites produced by lightning discharges associated with charge moment changes as small as 120 C·km (Hu et al., 2002) are not understood at present, and it is likely that details of the related physics are more complicated than simple scaling of the breakdown and thundercloud fields shown in Figure 6. In particular, Adachi et al. (2004) found that the number of sprite columns in each sprite event was proportional to the peak current intensity of positive cloud-to-ground lightning discharges (CGs) while the average vertical length of columns was proportional to the charge moment of the causative positive CGs. Recent studies of Gerken and Inan (2004) indicate that relatively faint and diffuse sprites confined to small altitude range are associated

with very high peak currents and short time duration of causative lightning discharges. Ohkubo et al. (2005) reported association of sprites with clusters of VLF radio atmospherics (sferics), similar to those observed previously in association with subionospheric signal perturbations referred to as "early/fast" VLF events (Johnson and Inan, 2000). These studies indicate a possible and not yet fully understood role of the time characteristics of the lightning currents in the initiation of sprites.

High speed imaging of sprites has captured their temporal development, indicating that most sprites are initiated with a bright column or streamers and followed by the upward and downward branching (Stanley et al., 1999; Stenbaek-Nielsen et al., 2000; Gerken and Inan, 2003; Moudry et al., 2003). On the other hand, sprite halos are observed typically preceding the occurrences of sprites (Barrington-Leigh et al., 2001; Wescott et al., 2001; Miyasato et al., 2002, 2003; Moudry et al., 2003; Gerken and Inan, 2003). It has recently been speculated that an enhancement of the electric field at the bottom of the sprite halo may create favorable conditions for subsequent streamer breakdown (Barrington-Leigh et al., 2001). The recent observations of early/fast VLF events by Moore et al. (2003) provide additional evidence for the electron density disturbances associated with sprite halo events.

Other proposed approaches to initiation of sprite streamers in very weak electric fields include localized inhomogeneities in the mesospheric medium (Moudry et al., 2003), electromagnetic pulses from horizontal lightning discharges forming localized peaks of electron density in the altitude range 75-85 km (Cho and Rycroft, 2001), and external triggers such as meteors or micrometeors (Suszcynsky et al., 1999; Wescott et al., 2001; Zabotin and Wright, 2001). We note that initiation of sprite streamers in low fields ($E<E_k$) requires strong conductivity enhancements comparable to conductivity of streamers themselves. At a typical sprite initiation altitude of 70 km the required electron density perturbations should be on the order of $10^6 \mathrm{cm}^{-3}$ (see Figure 8c). Cosmic rays contribute to the background ionization at these altitudes, however, the related electron densities are expected to be low even under conditions of relativistic runaway phenomena (i.e., $E_k>E>E_t$, Section 12.2.3) due to prohibitively long avalanche distances l_a of relativistic runaway electrons at low pressures (i.e., at 70 km l_a=50 m$\times(E_t/E)(N_o/N)\simeq$370 km assuming $E/E_t\simeq$2 (Gurevich and Zybin, 2001)).

12.5.3 Propagation of Sprite Streamers

The overall volumetric effects of sprites on the upper atmosphere can be evaluated using two and three dimensional phenomenological fractal models of streamer coronas (Pasko et al., 2000, 2001), and references therein (see Section 12.3.3). In this type of models the minimum fields required for positive

and negative streamer advancement at various pressures are specified externally as input parameters. It should be emphasized that these fields have not yet been determined at air pressures corresponding to sprite altitudes and the existing models employ a highly simplified assumption by using the ground level values scaled linearly with pressure (e.g., Pasko et al., 2000) (this assumption, contradicts to a limited amount existing experimental data on the subject, as will be discussed below). The determination of the minimum fields needed for propagation of streamers at low pressures represents one of the important tasks of the current sprite research. The information about these fields is needed for the correct evaluation of the total volume of atmosphere affected by sprite phenomenon as well as for evaluation of the possible role of sprites in establishing a direct path of electrical contact between the tropospheric and mesospheric/lower ionospheric regions (see Pasko et al., 2001, for references to relevant experimental data).

As it has already been discussed in Section 12.2.3 the minimum field required for the propagation of positive streamers in air at ground pressure (E_{cr}^{+}) has been extensively documented experimentally and usually stays close to the value 4.4 kV/cm (Allen and Ghaffar, 1995) which agrees well with recent results of numerical simulations of positive streamers (Babaeva and Naidis, 1997; Morrow and Lowke, 1997). The information about the absolute value of the similar field (E_{cr}^{-}) for the negative streamers at present is very limited. The existing sources indicate that this field is a factor of 2-3 times higher than the corresponding field for the positive streamers (Raizer, 1991, p. 361; Babaeva and Naidis, 1997).

The data on minimum fields required for propagation of streamers at pressures lower than atmospheric are very limited in currently available literature (e.g., Griffiths and Phelps, 1976; Aleksandrov and Bazelyan, 1996; Bazelyan and Raizer, 1998, p. 216). Although from the streamer similarity laws one generally would expect the minimum fields required for streamer propagation to scale with altitude proportionally to the air neutral density N, the actual scaling for the altitude range of sprites has not yet been verified experimentally. In experiments reported in Griffiths and Phelps (1976) and Bazelyan and Raizer (1998), p. 216, the measurements were performed for a set of relatively high pressures corresponding to altitudes $<$12 km, and the E_{cr}^{+} was found to drop with altitude faster than N. These deviations may be a manifestation of the effects, which are able to destroy the streamer similarity at high pressures (i.e., possibly related to the neutral gas heating and the three-body electron attachment) and which are not yet well understood at this time. On the other hand, the data presented by different authors remain controversial, and some studies of streamers indicate nearly linear scaling of E_{cr}^{+} with pressure (Aleksandrov and Bazelyan, 1996, and references cited therein).

12.5.4 Branching of Sprite Streamers

The complex morphology of sprites is well documented in existing literature (e.g., Stenbaek-Nielsen et al., 2000; Gerken and Inan, 2003; Moudry et al., 2003). Early video observations have revealed upward and downward branching structures in sprites (Sentman et al., 1996; Taylor and Clark, 1996; Stanley et al., 1996; Fukunishi et al., 1996a). Complex time dynamics with upward and downward propagating tree-like structures has also been reported during more recent high-speed video observations of sprites (Stanley et al., 1999; Stenbaek-Nielsen et al., 2000). The observed tree-like structures are likely to be related to the branching property of individual streamer channels. The upward (negative streamers) and downward (positive streamers) branching has been clearly seen in some of the sprites (Moudry et al., 2003; Gerken and Inan, 2003).

The branching phenomenon has received increasing attention in recent experimental and modeling studies of streamers at ground pressure (Popov, 2002; Arrayas et al., 2002; Rocco et al., 2002; Yi and Williams, 2002; van Veldhuizen and Rutgers, 2002; Ono and Oda, 2003; Akyuz et al., 2003; Hallac et al., 2003; Arrayas and Ebert, 2004; Pancheshnyi et al., 2005; Briels et al., 2005). Interest in these studies is largely motivated by numerous chemical applications of streamers, including treatment of large gas volumes for the purposes of pollution control and ozone production (e.g., van Veldhuizen, 2000, and references therein). The branching features of sprites (Gerken and Inan, 2003) and ground (van Veldhuizen and Rutgers, 2002) streamers are very similar, although their spatial scales are different by several orders of magnitude (i.e., decameter streamers in comparison with a fraction of millimeter ground streamers, as discussed in Section 12.3.4 and illustrated in Figure 8).

Finding the exact physical factors, which define the transverse spatial scale of a streamer, is a difficult task since simplified streamer models do not usually provide a characteristic spatial scale for the streamer radius (e.g., Raizer and Simakov, 1998, Bazelyan and Raizer, 1998, p. 277; Kulikovsky, 2000, and references cited therein). It has recently been demonstrated that negative streamers developing in high ambient fields, when no is pre-ionization available ahead of the streamer, are reaching an unstable "ideal conductivity" state with approximately equipotential and weakly curved head (Arrayas et al., 2002; Rocco et al., 2002). It was proposed that this new state exhibits a Laplacian instability, like that in viscous fingering, which leads to branching of the streamer (Arrayas et al., 2002; Rocco et al., 2002). However, the authors also pointed out that the branching of streamers does depend on the numerical discretization to certain degree. There still exists disagreement on whether the branching of model streamers is a pseudo-branching and is a consequence of a numerical instability (Pancheshnyi and Starikovskii, 2001, 2003), or correctly reflects the real splitting physics of streamers.

A limited set of modeling studies conducted by Liu and Pasko (2004) indicate that the maximum radius of the expanding streamers is predominantly controlled by the combination of the absorption cross section $\chi_{\min}$=3.5$\times 10^{-2}$ cm^{-1}Torr^{-1} of the molecular oxygen (O_2) at 1025 Å and the partial pressure of O_2 in air, p_{O_2}, and streamers exhibit branching when their radius becomes greater than $1/\chi_{\min} p_{O_2}$. Model results indicate a lower branching threshold radius for positive streamers in comparison with negative streamers, under otherwise identical ambient conditions. These results are in good agreement with recent results of high-speed photography of laboratory streamers in near-atmospheric pressure N_2/O_2 mixtures (Yi and Williams, 2002; van Veldhuizen and Rutgers, 2002; Ono and Oda, 2003) and similar morphology documented during recent telescopic and high-speed video observations of sprites (Moudry et al., 2003; Gerken and Inan, 2003). The importance of photoionization effects for the branching of streamers has also been noticed in the recent numerical study of ground streamers by Hallac et al. (2003). Following arguments presented in (Liu and Pasko, 2004) we note that non-similar reduction in photoelectron production at high pressures due to quenching of UV emitting excited states of N_2 is expected to lead to enhanced branching activity and smaller transverse scales of streamers at high pressures. Such behavior indeed was noted in recent experiments (Pancheshnyi et al., 2005; Briels et al., 2005).

The investigation of streamer splitting characteristics is still in the very preliminary stage. Although some pre-branching features, such as extremely high peak field and electron density in the head with a weak curvature, have been commonly observed in recent studies by several authors (Arrayas et al., 2002; Rocco et al., 2002; Liu and Pasko, 2004), the results on branching morphology reported by different research groups remain highly controversial (Kulikovsky, 2000; Pancheshnyi and Starikovskii, 2001; Kulikovsky, 2001, 2002; Ebert and Hundsdorfer, 2002; Hallac et al., 2003; Liu and Pasko, 2004). The documentation of exact branching conditions of positive and negative streamers in sprites constitutes one of the important tasks of the current TLE research.

12.5.5 Thermal Runaway Electrons in Streamer Tips in Sprites

As it has been already discussed in Section 12.3.4 the observed filamentary structures in sprites (Gerken and Inan, 2003) have recently been interpreted in terms of thin channels of ionization called streamers, which exhibit acceleration, expansion and branching (Liu and Pasko, 2004). The expanding streamers can reach a branching state for a wide range of applied electric fields and an extremely high peak field can be generated in the streamer tip immediately preceding the branching (Liu and Pasko, 2004) (see also discussion on streamer

branching in the previous section). The acceleration of electrons in tips of highly overvolted streamers (Babich, 1982) has been proposed for interpretation of X-ray radiation observed in experiments reported by Tarasova et al. (1974). It has also been proposed that the high electric fields in streamer tips can accelerate electrons to energies of several keV, initiating electron runaway in relatively low ambient electric fields $E \sim E_k$ (Pasko et al., 1998b), and references cited therein, where E_k is the conventional breakdown threshold field defined in Section 12.2.3. The peak charge moment changes of 3070 C·km (Hu et al., 2002) and 5950 C·km (Cummer and Füllekrug, 2001) corresponding to $E \simeq 2.3 E_k$ and $E \simeq 4.4 E_k$, respectively, at 70 km altitude, may create favorable conditions for the streamer tip runaway phenomena. It is known that X-ray emissions produced by corona discharges in high voltage equipment can be a serious personnel hazard (Roth, 1995, p. 256; Roth, 2001, pp. 48-49). The recently reported X-ray emissions observed in association with natural lightning stepped leaders and triggered lightning dart leaders (Moore et al., 2001; Dwyer et al., 2003, 2004b, 2005) may be related to the enhancement of electric field in the leader streamer zone (Dwyer et al., 2004a) leading to the generation of runaway electrons in streamer tips. The quantitative calculation of fluxes of thermal runaway electrons generated in streamer tips and evaluation of their overall importance in conventional lightning as well as in sprite phenomenon represents an example of another outstanding problem in sprite research. Since streamers can represent a robust source of runaway electrons, the related studies may also be relevant to gamma ray flashes of terrestrial origin (e.g., Smith et al., 2005), and references therein.

Acknowledgments

This research was supported by NSF ATM-0134838 grant to Penn State University.

Bibliography

Adachi, T., Fukunishi, H., Takahashi, Y., and Sato, M. (2004). Roles of the EMP and QE field in the generation of columniform sprites. *Geophys. Res. Lett.*, 31(4):doi:10.1029/2003GL019081.

Akyuz, M., Larsson, A., Cooray, V., and Strandberg, G. (2003). 3D simulations of streamer branching in air. *J. Electrostatics*, 59(115–141):doi: 10.1016/S0304–3886(03)00066–4.

Aleksandrov, N. L. and Bazelyan, E. M. (1996). Temperature and density effects on the properties of a long positive streamer in air. *J. Phys. D: Appl. Phys.*, 29:2873–2880.

Allen, N. L. and Ghaffar, A. (1995). The conditions required for the propagation of a cathode-directed positive streamer in air. *J. Phys. D: Appl. Phys.*, 28:331–337.

Armstrong, R. A., Shorter, J. A., Taylor, M. J., Suszcynsky, D. M., Lyons, W. A., and Jeong, L. S. (1998). Photometric measurements in the SPRITES' 95 and 96 campaigns of nitrogen second positive (399.8 nm) and first negative (427.8 nm) emission. *J. Atmos. Sol.-Terr. Phys.*, 60:787–799.

Armstrong, R. A., Suszcynsky, D. M., Lyons, W. A., and Nelson, T. E. (2000). Multi-color photometric measurements of ionization and energies in sprites. *Geophys. Res. Lett.*, 27:653–657.

Arrayas, M. and Ebert, U. (2004). Stability of negative ionization fronts: Regularization by electric screening? *Phys. Rev. E*, 69:doi:10.1103/PhysRevE .69.036214.

Arrayas, M., Ebert, U., and Hundsdorfer, W. (2002). Spontaneous branching of anode-directed streamers between planar electrodes. *Phys. Rev. Lett.*, 88:doi:10.1103/PhysRevLett.88.174502.

Babaeva, N. Y. and Naidis, G. V. (1997). Dynamics of positive and negative streamers in air in weak uniform electric fields. *IEEE Trans. Plasma Sci.*, 25:375–379.

Babich, L. P. (1982). A new type of ionization wave and the mechanism of polarization self-acceleration of electrons in gas discharge at high overvoltages. *Sov. Phys. Dokl.*, 27:215.

Babich, L. P. (2003). *High-energy phenomena in electric discharges in dense gases: Theory, experiment and natural phenomena*, volume 2 of *ISTC Science and Technology Series*. Futurepast, Arlington, Virginia.

Barrington-Leigh, C. P., Inan, U. S., and Stanley, M. (2001). Identification of sprites and elves with intensified video and broadband array photometry. *J. Geophys. Res.*, 106(A2):doi: 10.1029/ 2000JA000073.

Bazelyan, E. M. and Raizer, Y. P. (1998). *Spark discharge*. CRC Press, Boca Raton.

Bell, T. F., Pasko, V. P., and Inan, U. S. (1995). Runaway electrons as a source of red sprites in the mesosphere. *Geophys. Res. Lett.*, 22:2127–2131.

Blanc, E., Farges, T., Roche, R., Brebion, D., Hua, T., Labarthe, A., and Melnikov, V. (2004). Nadir observations of sprites from the International Space Station. *J. Geophys. Res.*, 109(A2):doi:10.1029/2003JA009972.

Boccippio, D. J., Williams, E. R., Heckman, S. J., Lyons, W. A., Baker, I. T., and Boldi, R. (1995). Sprites, ELF transients, and positive ground strokes. *Science*, 269:1088–1091.

Boeck, W. L., O. H. Vaughan, Jr. and R. J. Blakeslee, Vonnegut, B., Brook, M., and McKune, J. (1995). Observations of lightning in the stratosphere. *J. Geophys. Res.*, 100:1465–1475.

Briels, T. M. P., van Veldhuizen, E. M., and Ebert, U. (2005). Branching of positive discharge streamers in air at varying pressures. *IEEE Trans. Plasma Sci.*, 33(2):264–265.

Bucsela, E., Morrill, J., Heavner, M., Siefring, C., Berg, S., Hampton, D., Moudry, D., Wescott, E., and Sentman, D. (2003). $N_2(B^3\Pi_g)$ and $N_2^+(A^2\Pi_u)$ vibrational distributions observed in sprites. *J. Atmos. Sol.-Terr. Phys.*, 65:583–590.

Cho, M. and Rycroft, M. J. (2001). Non-uniform ionisation of the upper atmosphere due to the electromagnetic pulse from a horizontal lightning discharge. *J. Atmos. Sol.-Terr. Phys.*, 63:559–580.

Cooray, G. V. (2003). *The lightning flash*. IEE, London, UK.

Cummer, S. A. (2003). Current moment in sprite-producing lightning. *J. Atmos. Sol.-Terr. Phys.*, 65(499–508):doi:10.1016/S1364–6826(02)00318–8.

Cummer, S. A. and Füllekrug, M. (2001). Unusually intense continuing current in lightning produces delayed mesospheric breakdown. *Geophys. Res. Lett.*, 28:495–499.

Cummer, S. A., Inan, U. S., Bell, T. F., and Barrington-Leigh, C. P. (1998). ELF radiation produced by electrical currents in sprites. *Geophys. Res. Lett.*, 25:1281–1285.

Cummer, S. A., Zhai, Y., Hu, W., Smith, D. M., Lopez, L. I., and Stanley, M. A. (2005). Measurements and implications of the relationship between lightning and terrestrial gamma-ray flashes. *Geophys. Res. Lett.*, 32(L08811):doi:10.1029/2005GL022778.

Dhali, S. K. and Williams, P. F. (1987). Two-dimensional studies of streamers in gases. *J. Appl. Phys.*, 62:4696–4707.

Dwyer, J. R. (2003). A fundamental limit on electric fields in air. *Geophys. Res. Lett.*, 30(20):doi:10.1029/2003GL017781.

Dwyer, J. R. (2004). Implications of X-ray emission from lightning. *Geophys. Res. Lett.*, 31(L12102):doi: 10.1029/2004GL019795.

Dwyer, J. R. (2005). Gamma-ray events from thunderclouds. In *2005 Seminar Series on Terrestrial Gamma Ray Flashes and Lightning Associated Phenomena*, Space Science Laboratory, University of California, Berkeley.

Dwyer, J. R., Rassoul, H. K., Al-Dayeh, M., Caraway, L., Chrest, A., Wright, B., Kozak, E., Jerauld, J., Uman, M. A., Rakov, V. A., Jordan, D. M., and Rambo, K. J. (2005). X-ray bursts associated with leader steps in cloud-to-ground lightning. *Geophys. Res. Lett.*, 32:doi:10.1029/2004GL021782.

Dwyer, J. R., Rassoul, H. K., Al-Dayeh, M., Caraway, L., Wright, B., Chrest, A., Uman, M. A., Rakov, V. A., Rambo, K. J., Jordan, D. M., Jerauld, J., and Smyth, C. (2004a). A ground level gamma-ray burst observed in association with rocket-triggered lightning. *Geophys. Res. Lett.*, 31(L05119):doi:10.1029/2003GL018771.

Dwyer, J. R., Rassoul, H. K., Al-Dayeh, M., Caraway, L., Wright, B., Chrest, A., Uman, M. A., Rakov, V. A., Rambo, K. J., Jordan, D. M., Jerauld, J., and Smyth, C. (2004b). Measurements of X-ray emission from rocket-triggered lightning. *Geophys. Res. Lett.*, 31(L05118):doi: 10.1029/2003GL018770.

Dwyer, J. R., Uman, M. A., Rassoul, H. K., Al-Dayeh, M., Caraway, L., Jerauld, J., Rakov, V. A., Jordan, D. M., Rambo, K. J., Corbin, V., and Wright, B. (2003). Energetic radiation produced during rocket-triggered lightning. *Science*, 299:694–697.

Eack, K. B., Beasley, W. H., Rust, W. D., Marshall, T. C., and Stolzenburg, M. (1996a). Initial results from simultaneous observation of X rays and electric fields in a thunderstorm. *J. Geophys. Res.*, 101:29637–29640.

Eack, K. B. and W. H. Beasley, Rust, W. D., Marshall, T. C., and Stolzenburg, M. (1996b). X-ray pulses observed above a mesoscale convective system. *Geophys. Res. Lett.*, 23:2915–2918.

Ebert, U. and Hundsdorfer, W. (2002). Comment on "Spontaneous branching of anode-directed streamers between planar electrodes" - Reply. *Phys. Rev. Lett.*, 89(22):doi: 10.1103/ PhysRevLett. 89.229402.

Farges, T., Blanc, E., Pichon, A. Le, Neubert., T., and Allin, T. H. (2005). Identification of infrasound produced by sprites during the Sprite2003 campaign. *Geophys. Res. Lett.*, 32(1):doi:10.1029/2004GL021212.

Fishman, G. J., Bhat, P. N., Mallozzi, R., Horack, J. M., Koshut, T., Kouveliotou, C., Pendleton, G. N., Meegan, C. A., Wilson, R. B., Paciesas, W. S., Goodman, S. J., and Christian, H. J. (1994). Discovery of intense gamma-ray flashes of atmospheric origin. *Science*, 264:1313–1316.

Franz, R. C., Nemzek, R. J., and Winckler, J. R. (1990). Television image of a large upward electrical discharge above a thunderstorm system. *Science*, 249:48–51.

Frey, H., Mende, S., Hsu, R. R., Su, H. T., Chen, A., Lee, L. C., Fukunishi, H., and Takahashi, Y. (2004). The spectral signature of transient luminous events (TLE, sprite, elve, halo) as observed by ISUAL. *Eos Trans. AGU - Fall Meet. Suppl.*, 85(47):AE51A–05. Abstract.

Fukunishi, H., Takahashi, Y., Fujito, M., Wanatabe, Y., and Sakanoi, S. (1996a). Fast imaging of elves and sprites using a framing/streak camera and a multi-anode array photometer. *Eos Trans. AGU - Fall Meet. Suppl.*, 77(46):F60.

Fukunishi, H., Takahashi, Y., Kubota, M., Sakanoi, K., Inan, U. S., and Lyons, W. A. (1996b). Elves: Lightning-induced transient luminous events in the lower ionosphere. *Geophys. Res. Lett.*, 23(16):2157–2160.

Fukunishi, H., Takahashi, Y., Uchida, A., Sera, M., Adachi, K., and Miyasato, R. (1999). Occurrences of sprites and elves above the Sea of Japan near Hokuriku in winter. *Eos Trans. AGU - Fall Meet. Suppl*, 80:F217.

Füllekrug, M. and Constable, S. (2000). Global triangulation of intense lightning discharges. *Geophys. Res. Lett.*, 27:333–336.

Füllekrug, M., Moudry, D. R., Dawes, G., and Sentman, D. D. (2001). Mesospheric sprite current triangulation. *J. Geophys. Res.*, 106:20189–20194.

Füllekrug, M. and Reising, S. C. (1998). Excitation of Earth-ionosphere cavity resonances by sprite-associated lightning flashes. *Geophys. Res. Lett.*, 25:4145–4148.

Gallimberti, I., Bacchiega, G., Bondiou-Clergerie, A., and Lalande, P. (2002). Fundamental processes in long air gap discharges. *Compt. Rend. Phys.*, 3:1335–1359.

Gerken, E. A. and Inan, U. S. (2002). A survey of streamer and diffuse glow dynamics observed in sprites using telescopic imagery. *J. Geophys. Res.*, 107(A11):doi:10.1029/2002JA009248.

Gerken, E. A. and Inan, U. S. (2003). Observations of decameter-scale morphologies in sprites. *J. Atmos. Sol.-Terr. Phys*, 65(567–572):doi:10.1016/ S1364–6826(02)00333–4.

Gerken, E. A. and Inan, U. S. (2004). Comparison of photometric measurements and charge moment estimations in two sprite-producing storms. *Geophys. Res. Lett.*, 31(L03107):doi: 10.1029/ 2003GL018751.

Gerken, E. A. and Inan, U. S. (2005). Streamers and diffuse glow observed in upper atmospheric electrical discharges. *IEEE Trans. Plsama Sci.*, 33(2):282–283.

Gerken, E. A., Inan, U. S., and Barrington-Leigh, C. P. (2000). Telescopic imaging of sprites. *Geophys. Res. Lett.*, 27:2637–2640.

Grange, F., Soulem, N., Loiseau, J. F., and Spyrou, N. (1995). Numerical and experimental-determination of ionizing front velocity in a DC point-to-plane corona discharge. *J. Phys. D: Appl. Phys.*, 28:1619–1629.

Griffiths, R. F. and Phelps, C. T. (1976). The effects of air pressure and water vapour content on the propagation of positive corona streamers, and their implications to lightning initiation. *Quart. J. Roy. Met. Soc.*, 102:419–426.

Gurevich, A. V., Milikh, G. M., and Roussel-Dupré, R. (1992). Runaway electron mechanism of air breakdown and preconditioning during a thunderstorm. *Phys. Lett. A*, 165:463–468.

Gurevich, A. V. and Zybin, K. P. (2001). Runaway breakdown and electric discharges in thunderstorms. *Phys.-Uspekhi*, 44:1119–1140.

Hallac, A., Georghiou, G. E., and Metaxas, A. C. (2003). Secondary emission effects on streamer branching in transient non-uniform short-gap discharges. *J. Phys. D: Appl. Phys.*, 36:doi:10.1088/0022–3727/36/20/011.

Hampton, D. L., Heavner, M. J., Wescott, E. M., and Sentman, D. D. (1996). Optical spectral characteristics of sprites. *Geophys. Res. Lett.*, 23:89–93.

Hardman, S. F., Dowden, R. L., Brundell, J. B., Bahr, L., Kawasaki, Z., and Rodger, C. J. (1998). Sprites in Australia's Northern Territory. *Eos Trans. AGU - Fall Meet. Suppl.*, 79:F135.

Hardman, S. F., Dowden, R. L., Brundell, J. B., Bahr, L., Kawasaki, Z., and Rodger, C. J. (2000). Sprite observations in the Northern Territory of Australia. *J. Geophys. Res.*, 105(D4):4689–4698.

Hayakawa, M., Nakamura, T., Hobara, Y., and Williams, E. (2004). Observations of sprites over the Sea of Japan and conditions for lightning-induced sprites in winter. *J. Geophys. Res.*, 109:doi:10.1029/2003JA009905.

Heavner, M. J., Hampton, D., Sentman, D., and Wescott, E. (1995). Sprites over Central and South America - Fall Meet. Suppl. *Eos Trans. AGU*, 76(46):F115.

Heavner, M. J., Sentman, D. D., Moudry, D. R., and Wescott, E. M. (2000). Sprites, blue jets, and elves: Optical evidence of energy transport across the stratopause. In Siskind, D.E., Eckermann, S.D., and Summers, M.E., editors, *Atmospheric Science Across the Stratopause*, volume 123 of *Geophysical Monograph Series*, pages 69–82. AGU.

Hobara, Y., Iwasaki, N., Hayashida, T., Hayakawa, M., Ohta, K., and Fukunishi, H. (2001). Interrelation between ELF transients and ionospheric disturbances in association with sprites and elves. *Geophys. Res. Lett.*, 28(5):doi:10.1029/2000GL003795.

Holzworth, R. H., McCarthy, M. P., Thomas, J. N., Chinowsky, T. M., Taylor, M. J., and Pinto, O. (2003). Strong electric fields from positive lightning strokes in the stratosphere: Implications for sprites - Fall Meet. Suppl., Abstract. *Eos Trans. AGU*, 84(46):AE51A–01.

Hsu, R. R., Su, H. T., Chen, A. B., Lee, L. C., Asfur, M., Price, C., and Yair, Y. (2003). Transient luminous events in the vicinity of Taiwan. *J. Atmos. Sol.-Terr. Phys.*, 65(5):561–566.

Hu, W. Y., Cummer, S. A., and Lyons, W. A. (2002). Lightning charge moment changes for the initiation of sprites. *Geophys. Res. Lett.*, 29(8):doi: 10.1029/2001GL014593.

ICRU (1984). International commission on radiation units and measurements, stopping powers for electrons and positrons. ICRU Rep. 37. Tables 8.1 and 12.4, Bethesda, Md.

Inan, U. S. (2005). Gamma rays made on Earth. *Science*, 307:1054–1055.

Inan, U. S., Barrington-Leigh, C., Hansen, S., Glukhov, V. S., Bell, T. F., and Rairden, R. (1997). Rapid lateral expansion of optical luminosity in lightning-induced ionospheric flashes referred to as 'elves'. *Geophys. Res. Lett.*, 24(5):583–586.

Inan, U. S., Cohen, M., and Said, R. (2005). Terrestrial gamma ray flashes and VLF radio atmospherics. In *2005 Seminar Series on Terrestrial Gamma Ray Flashes and Lightning Associated Phenomena*, Space Science Laboratory, University of California, Berkeley.

Inan, U. S., Reising, S. C., Fishman, G. J., and Horack, J. M. (1996). On the association of terrestrial gamma-ray bursts with lightning and implications for sprites. *Geophys. Res. Lett.*, 23:1017–1020.

Israelevich, P. L., Yair, Y., Devir, A. D., Joseph, J. H., Levin, Z., Mayo, I., Moalem, M., Price, C., Ziv, B., and Sternlieb, A. (2004). Transient airglow enhancements observed from the Space Shuttle Columbia during the MEIDEX sprite campaign. *Geophys. Res. Lett.*, 31(L06124):doi: 10.1029/ 2003GL019110.

Johnson, M. P. and Inan, U. S. (2000). Sferic clusters associated with Early/Fast VLF events. *Geophys. Res. Lett.*, 27:1391–1394.

Kulikovsky, A. A. (1997). Production of chemically active species in the air by a single positive streamer in a nonuniform field. *IEEE Trans. Plasma Sci.*, 25:439–446.

Kulikovsky, A. A. (2000). The role of photoionization in positive streamer dynamics. *J. Phys. D: Appl. Phys.*, 33:1514–1524.

Kulikovsky, A. A. (2001). Reply to comment on 'The role of photoionization in positive streamer dynamics'. *J. Phys. D: Appl. Phys.*, 34:251–252.

Kulikovsky, A. A. (2002). Comment on "Spontaneous branching of anode-directed streamers between planar electrodes". *Phys. Rev. Lett.*, 89(22):doi: 10.1103/ PhysRevLett.89.229401.

Kunhardt, E. E. and Tzeng, Y. (1988). Development of an electron avalanche and its transition into streamers. *Phys. Rev. A.*, 38:1410–1421.

Kutsyk, I. M. and Babich, L. P. (1999). Spatial structure of optical emissions in the model of gigantic upward atmospheric discharges with participation of runaway electrons. *Phys. Lett. A*, 253:75–82.

Lehtinen, N. G., Bell, T. F., Pasko, V. P., and Inan, U. S. (1997). A two-dimensional model of runaway electron beams driven by quasi-electrostatic thundercloud fields. *Geophys. Res. Lett.*, 24:2639–2642.

Lehtinen, N. G., Inan, U. S., and Bell, T. F. (1999). Monte Carlo simulation of runaway MeV electron breakdown with application to red sprites and terrestrial gamma ray flashes. *J. Geophys. Res.*, 104:24699–24712.

Lehtinen, N. G., Inan, U. S., and Bell, T. F. (2000). Trapped energetic electron curtains produced by thunderstorm driven relativistic runaway electrons. *Geophys. Res. Lett.*, 27:1095–1098.

Lehtinen, N. G., Inan, U. S., and Bell, T. F. (2001). Effects of thunderstorm-driven runaway electrons in the conjugate hemisphere: Purple sprites, ionization enhancements, and gamma rays. *J. Geophys. Res.*, 106:28841–28856.

Lehtinen, N. G., Walt, M., Inan, U. S., Bell, T. F., and Pasko, V. P. (1996). Gamma-ray emission produced by a relativistic beam of runaway electrons accelerated by quasi-electrostatic thundercloud fields. *Geophys. Res. Lett.*, 23:2645–2648.

Lieberman, M. A. and Lichtenberg, A. J. (1994). *Principles of plasma discharges and materials processing*. John Wiley & Sons Inc.

Liszka, L. (2004). On the possible infrasound generation by sprites. *J. Low Freq. Noise, Vibration and Active Cont.*, 23(2):85–93.

Liu, N. and Pasko, V. P. (2004). Effects of photoionization on propagation and branching of positive and negative streamers in sprites. *J. Geophys. Res.*, 109:A04301, doi:10.1029/2003JA010064. (see also Liu, N., and V. P. Pasko, Correction to "Effects of photoionization on propagation and branching of positive and negative streamers in sprites," *J. Geophys. Res., 109,* A09306, doi:10.1029/2004JA010692, 2004).

Liu, N. and Pasko, V. P. (2005). Molecular nitrogen LBH band system far-UV emissions of sprite streamers. *Geophys. Res. Lett.*, 32:doi:10.1029/2004GL022001.

Loeb, L. B. and Meek, J. M. (1940). The mechanism of spark discharge in air at atmospheric pressure. *J. Appl. Phys.*, 11:438–447.

Lyons, W. A. (1996). Sprite observations above the U.S. high plains in relation to their parent thunderstorm systems. *J. Geophys. Res.*, 101(29):641.

Lyons, W. A., Nelson, T. E., Armstrong, R. A., Pasko, V. P., and Stanley, M. A. (2003a). Upward electrical discharges from thunderstorm tops. *Bull. Am. Met. Soc.*, 84(4):445–454.

Lyons, W. A., Nelson, T. E., Williams, E. R., Cummer, S. A., and Stanley, M. A. (2003b). Characteristics of sprite-producing positive cloud-to-ground lightning during the 19 July 2000 STEPS mesoscale convective systems. *Mon. Wea. Rev.*, 131:2417–2427.

Marshall, R. A. and Inan, U. S. (2005). High-speed telescopic imaging of sprites. *Geophys. Res. Lett.*, 32(L05804):doi:10.1029/2004GL021988.

Marshall, T. C., McCarthy, M. P., and Rust, W. D. (1995). Electric-field magnitudes and lightning initiation in thunderstorms. *J. Geophys. Res.*, 100:7097–7103.

Marshall, T. C. and Rust, W. D. (1993). Two types of vertical electrical structures in stratiform precipitation regions of mesoscale convective systems. *Bull. Am. Met. Soc.*, 74:2159.

Marshall, T. C., Stolzenburg, M., Maggio, C. R., Coleman, L. M., Krehbiel, P. R., Hamlin, T., Thomas, R. J., and Rison, W. (2005). Observed electric fields associated with lightning initiation. *Geophys. Res. Lett.*, 32(L03813):doi:10.1029/2004GL021802.

Marshall, T. C., Stolzenburg, M., and Rust, W. D. (1996). Electric field measurements above mesoscale convective systems. *J. Geophys. Res.*, 101:6979–6996.

Marshall, T. C., Stolzenburg, M., Rust, W. D., Williams, E. R., and Boldi, R. (2001). Positive charge in the stratiform cloud of a mesoscale convective system. *J. Geophys. Res.*, 106:1157–1163.

McCarthy, M. P. and Parks, G. K. (1992). On the modulation of X-ray fluxes in thunderstorms. *J. Geophys. Res.*, 97:5857–5864.

McHarg, M. G., Haaland, R. K., Moudry, D. R., and Stenbaek-Nielsen, H. C. (2002). Altitude-time development of sprites. *J. Geophys. Res.*, 107(A11):doi:10.1029/2001JA000283.

Mende, S., Frey, H., R. R. Hsu, H. T. Su, Chen, A., Lee, L. C., Fukunishi, H., and Takahashi, Y. (2004). Sprite imaging results from the ROCSAT-2 ISUAL instrument. *Eos. Trans. AGU, Fall Meet. Suppl., Abstract AE51A-02*, 85(47).

Mende, S. B., Rairden, R. L., Swenson, G. R., and Lyons, W. A. (1995). Sprite spectra: $N_2$1PG band identification. *Geophys. Res. Lett.*, 22:2633–2637.

Milikh, G. M., Guzdar, P. N., and Sharma, A. S. (2005). Gamma ray flashes due to plasma processes in the atmosphere: Role of whistler waves. *J. Geophys. Res.*, 110(A02308):doi: 10.1029/ 2004JA010681.

Miyasato, R., Fukunishi, H., Takahashi, Y., and Taylor, M. J. (2003). Energy estimation of electrons producing sprite halos using array photometer data. *J. Atmos. Sol.-Terr. Phys.*, 65:573–581.

Miyasato, R., Taylor, M. J., Fukunishi, H., and Stenbaek-Nielsen, H. C. (2002). Statistical characteristics of sprite halo events using coincident photometric and imaging data. *Geophys. Res. Lett.*, 29(21):doi:10.1029/2001GL014480.

Moore, C. B., Eack, K. B., Aulich, G. D., and Rison, W. (2001). Energetic radiation associated with lightning stepped-leaders. *Geophys. Res. Lett.*, 28:2141–2144.

Moore, R. C., Barrington-Leigh, C. P., Inan, U. S., and Bell, T. F. (2003). Early/fast VLF events produced by electron density changes associated with sprite halos. *J. Geophys. Res.*, 108(A10):doi:10.1029/2002JA009816.

Morrill, J., Bucsela, E., Siefring, C., Heavner, M., Berg, S., Moudry, D., Slinker, S., Fernsler, R., Wescott, E., Sentman, D., and Osborne, D. (2002). Electron energy and electric field estimates in sprites derived from ionized and neutral N_2 emissions. *Geophys. Res. Lett.*, 29(10):doi: 10.1029/ 2001GL014018.

Morrill, J. S., Bucsela, E. J., Pasko, V. P., Berg, S. L., Benesch, W. M., Wescott, E. M., and Heavner, M. J. (1998). Time resolved N_2 triplet state vibrational populations and emissions associated with red sprites. *J. Atmos. Sol.-Terr. Phys.*, 60:811–829.

Morrow, R. and Lowke, J. J. (1997). Streamer propagation in air. *J. Phys. D: Appl. Phys.*, 30:614–627.

Moudry, D. R., Stenbaek-Nielsen, H. C., Sentman, D. D., and Wescott, E. M. (2002). Velocities of sprite tendrils. *Geophys. Res. Lett.*, 29(20):1992doi:10.1029/2002GL015682.

Moudry, D. R., Stenbaek-Nielsen, H. C., Sentman, D. D., and Wescott, E. M. (2003). Imaging of elves, halos and sprite initiation at 1 ms time resolution. *J. Atmos. Sol.-Terr. Phys.*, 65(509–518):doi:10.1016/S1364–6826(02)00323–1.

Neubert, T. (2003). On sprites and their exotic kin. *Science*, 300:747–749.

Neubert, T., Allin, T. H., Stenbaek-Nielsen, H., and Blanc, E. (2001). Sprites over Europe. *Geophys. Res. Lett.*, 28(18):doi:10.1029/2001GL013427.

Niemeyer, L., Ullrich, L., and Wiegart, N. (1989). The mechanism of leader breakdown in electronegative gases. *IEEE Trans. Electr. Insul.*, 24:309–324.

Ohkubo, A., Fukunishi, H., Takahashi, Y., and Adachi, T. (2005). VLF/ELF sferic evidence for in-cloud discharge activity producing sprites. *Geophys. Res. Lett.*, 32(L04812):doi: 10.1029/ 2004GL021943.

Ono, R. and Oda, T. (2003). Formation and structure of primary and secondary streamers in positive pulsed corona discharge effect of oxygen concentration and applied voltage. *J. Phys. D: Appl. Phys.*, 36(1952–1958):doi:10.1088/0022–3727/36/16/306.

Opal, C. B., Peterson, W. K., and Beaty, E. C. (1971). Measurements of secondary-electron spectra produced by electron impact ionization of a number of simple gases. *J. Chem. Phys.*, 55:4100–4106.

Pancheshnyi, S. V., Nudnova, M., and Starikovskii, A. Y. (2005). Development of a cathode-directed streamer discharge in air at different pressures: Experiment and comparison with direct numerical simulation. *Phys. Rev. E*, 71(016407):doi:10.1103/PhysRevE.71.016407.

Pancheshnyi, S. V. and Starikovskii, A. Y. (2001). Comments on 'The role of photoionization in positive streamer dynamics'. *J. Phys. D: Appl. Phys.*, 34:248–250.

Pancheshnyi, S. V. and Starikovskii, A. Y. (2003). Two-dimensional numerical modelling of the cathode-directed streamer development in a long gap at high voltage. *J. Phys. D: Appl. Phys.*, 36(2683–2691):doi:10.1088/0022–3727/36/21/014.

Pasko, V. P. (2003a). Dynamics of streamer-to-leader transition in transient luminous events between thunderstorm tops and the lower ionosphere. *Eos Trans. AGU - Fall Meet. Suppl.*, 84(46):AE41B–05. Abstract.

Pasko, V. P. (2003b). Electric jets. *Nature*, 423:927–929.

Pasko, V. P. and George, J. J. (2002). Three-dimensional modeling of blue jets and blue starters. *J. Geophys. Res.*, 107(A12):doi:10.1029/2002JA009473.

Pasko, V. P., Inan, U. S., and Bell, T. F. (1998a). Mechanism of ELF radiation from sprites. *Geophys. Res. Lett.*, 25:3493–3496.

Pasko, V. P., Inan, U. S., and Bell, T. F. (1998b). Spatial structure of sprites. *Geophys. Res. Lett.*, 25:2123–2126.

Pasko, V. P., Inan, U. S., and Bell, T. F. (1999). Mesospheric electric field transients due to tropospheric lightning discharges. *Geophys. Res. Lett.*, 26:1247–1250.

Pasko, V. P., Inan, U. S., and Bell, T. F. (2000). Fractal structure of sprites. *Geophys. Res. Lett.*, 27:497–500.

Pasko, V. P., Inan, U. S., and Bell, T. F. (2001). Mesosphere-troposphere coupling due to sprites. *Geophys. Res. Lett.*, 28:3821–3824.

Pasko, V. P., Inan, U. S., Bell, T. F., and Taranenko, Y. N. (1997). Sprites produced by quasi-electrostatic heating and ionization in the lower ionosphere. *J. Geophys. Res.*, 102:4529–4561.

Pasko, V. P., Stanley, M. A., Mathews, J. D., Inan, U. S., and Wood, T. G. (2002a). Electrical discharge from a thundercloud top to the lower ionosphere. *Nature*, 416:152–154. http://pasko.ee.psu.edu/Nature/.

Pasko, V. P., Stanley, M. A., Mathews, J. D., Inan, U. S., Wood, T. G., Cummer, S. A., Williams, E. R., and Heavner, M. J. (2002b). Observations of sprites above Haiti/Dominican Republic thunderstorms from Arecibo Observatory, Puerto Rico. *Eos Trans. AGU - Fall Meet. Suppl.*, 83(47):A62D–01. Abstract.

Pasko, V. P. and Stenbaek-Nielsen, H. C. (2002). Diffuse and streamer regions of sprites. *Geophys. Res. Lett.*, 29(A10):doi:10.1029/2001GL014241.

Petrov, N. I., Avanskii, V. R., and Bombenkova, N. V. (1994). Measurement of the electric field in the streamer zone and in the sheath of the channel of a leader discharge. *Tech. Phys.*, 39:546–551.

Petrov, N. I. and Petrova, G. N. (1993). Physical mechanisms for intracloud lightning discharges. *Tech. Phys.*, 38:287.

Petrov, N. I. and Petrova, G. N. (1999). Physical mechanisms for the development of lightning discharges between a thundercloud and the ionosphere. *Tech. Phys.*, 44:472–475.

Pinto Jr., O., Saba, M. M. F., Pinto, I. R. C. A., Tavares, F. S. S., Naccarato, K. P., Solorzano, N. N., Taylor, M. J., Pautet, P. D., and Holzworth, R. H. (2004). Thunderstorm and lightning characteristics associated with sprites in Brazil. *Geophys. Res. Lett.*, 31(L13103):doi:10.1029/2004GL020264.

Popov, N. A. (2002). Spatial structure of the branching streamer channels in a corona discharge. *Plasma. Phys. Rep.*, 28(7):doi:10.1134/1.1494061.

Price, C., Greenberg, E., Yair, Y., Satori, G., Bor, J., Fukunishi, H., Sato, M., Israelevich, P., Moalem, M., Devir, A., Levin, Z., Joseph, J. H., Mayo, I., Ziv, B., and Sternlieb, A. (2004). Ground-based detection of TLE-producing intense lightning during the MEIDEX mission on board the Space Shuttle Columbia,. *Geophys. Res. Lett.*, 31(L20107):doi:10.1029/2004GL020711.

Raizer, Y. P. (1991). *Gas discharge physics*. Springer-Verlag, Berlin Heidelberg.

Raizer, Y. P., Milikh, G. M., Shneider, M. N., and Novakovski, S. V. (1998). Long streamers in the upper atmosphere above thundercloud. *J. Phys. D: Appl. Phys.*, 31:3255–3264.

Raizer, Y. P. and Simakov, A. N. (1998). Main factors determining the radius of the head of a long streamer and the maximum electric field near the head. *Plasma. Phys. Rep.*, 24:700–706.

Rakov, V. A. and Uman, M. A. (2003). *Lightning physics and effects*. Cambridge University Press.

Reising, S. C., Inan, U. S., and Bell, T. F. (1999). ELF sferic energy as a proxy indicator for sprite occurrence. *Geophys. Res. Lett.*, 26:987–990.

Rocco, A., Ebert, U., and Hundsdorfer, W. (2002). Branching of negative streamers in free flight. *Phys. Rev. E*, 66:doi:10.1103/PhysRevE.66.035102.

Roth, R. J. (1995). *Industrial plasma engineering*, volume 1: Principles. IOP Publishing Ltd.

Roth, R. J. (2001). *Industrial plasma engineering*, volume 2: Applications to nonthermal plasma processing. IOP Publishing Ltd.

Roussel-Dupré, R. and Gurevich, A. V. (1996). On runaway breakdown and upward propagating discharges. *J. Geophys. Res.*, 101:2297–2311.

Roussel-Dupré, R., Gurevich, A. V., Tunnell, T., and Milikh, G. M. (1994). Kinetic-theory of runaway air breakdown. *Phys. Rev. E*, 49:2257–2271.

Roussel-Dupré, R., Symbalisty, E., Taranenko, Y., and Yukhimuk, V. (1998). Simulations of high-altitude discharges initiated by runaway breakdown. *J. Atmos. Sol.-Terr. Phys.*, 60:917–940.

Rowland, H. L. (1998). Theories and simulations of elves, sprites and blue jets. *J. Atmos. Sol.-Terr. Phys.*, 60:831–844.

Sato, M. and Fukunishi, H. (2003). Global sprite occurrence locations and rates derived from triangulation of transient Schumann resonance events. *Geophys. Res. Lett.*, 30(16):doi: 10.1029/ 2003GL017291.

Sentman, D. D., Wescott, E. M., Heavner, M. J., and Moudry, D. R. (1996). Observations of sprite beads and balls. *Eos Trans. AGU - Fall Meet. Suppl*, 77.

Sentman, D. D., Wescott, E. M., Osborne, D. L., Hampton, D. L., and Heavner, M. J. (1995). Preliminary results from the Sprites94 campaign: Red sprites. *Geophys. Res. Lett.*, 22:1205–1208.

Shepherd, T. R., Rust, W. D., and Marshall, T. C. (1996). Electric fields and charges near 0°C in stratiform clouds. *Mon. Wea. Rev.*, 124:919–938.

Smith, D. M., Lopez, L. I., Lin, R. P., and Barrington-Leigh, C. P. (2005). Terrestrial gamma-ray flashes observed up to 20 MeV. *Science*, 307:1085–1088.

Stanley, M., Krehbiel, P., Brook, M., Moore, C., Rison, W., and Abrahams, B. (1999). High speed video of initial sprite development. *Geophys. Res. Lett.*, 26:3201–3204.

Stanley, M., Krehbiel, P., Brook, M., Rison, W., Moore, C., and Vaughan, O. H. (1996). Observations of sprites and jets from Langmuir Laboratory, New Mexico. *Eos Trans. AGU - Fall Meet. Suppl*, 77(46):F69.

Stenbaek-Nielsen, H. C., Moudry, D. R., Wescott, E. M., Sentman, D. D., and Sabbas, F. T. Sao (2000). Sprites and possible mesospheric effects. *Geophys. Res. Lett.*, 27:3827–3832.

Su, H., Huang, T., Kuo, C., Chen, A. C., Hsu, R., Mende, S. B., Frey, H. U., Fukunishi, H., Takahashi, Y., and Lee, L. (2004). Global distribution of TLEs based on the preliminary ISUAL data. *Eos. Trans. AGU - Fall Meet. Suppl.*, 85(47):AE51A–03.

Su, H. T., Hsu, R. R., Chen, A. B., Lee, Y. J., and Lee, L. C. (2002). Observation of sprites over the Asian continent and over oceans around Taiwan. *Geophys. Res. Lett.*, 29(4):doi:10.1029/2001GL013737.

Su, H. T., Hsu, R. R., Chen, A. B., Wang, Y. C., Hsiao, W. S., Lai, W. C., Lee, L. C., Sato, M., and Fukunishi, H. (2003). Gigantic jets between a thundercloud and the ionosphere. *Nature*, 423:974–976.

Sukhorukov, A. I. and Stubbe, P. (1998). Problems of blue jet theories. *J. Atmos. Sol.-Terr. Phys.*, 60:725–732.

Suszcynsky, D. M., Roussel-Dupré, R., Lyons, W. A., and Armstrong, R. A. (1998). Blue-light imagery and photometry of sprites. *J. Atmos. Sol.-Terr. Phys.*, 60:801–809.

Suszcynsky, D. M., Strabley, R., Roussel-Dupré, R., Symbalisty, E. M. D., Armstrong, R. A., Lyons, W. A., and Taylor, M. (1999). Video and photometric observations of a sprite in coincidence with a meteor-triggered jet event. *J. Geophys. Res.*, 104(D24):doi: 10.1029/ 1999JD900962.

Symbalisty, E. M. D., Roussel-Dupré, R. A., and Yukhimuk, V. A. (1998). Finite volume solution of the relativistic Boltzmann equation for electron avalanche studies. *IEEE Trans. Plasma Sci.*, 26:1575–1582.

Takahashi, Y., Fujito, M., Watanabe, Y., Fukunishi, H., and Lyons, W A. (2000). Temporal and spatial variations in the intensity ratio of N-2 1st and 2nd positive bands in SPRITES. *Advances in Space Research*, 26(8):1205–1208.

Taranenko, Y. N. and Roussel-Dupré, R. (1996). High altitude discharges and gamma ray flashes: A manifestation of runaway air breakdown. *Geophys. Res. Lett.*, 23:571–574.

Tarasova, L. V., Khudyakova, L. N., Loiko, T. V., and Tsukerman, V. A. (1974). Fast electrons and X rays from nanosecond gas discharges at 0.1-760 Torr. *Sov. Phys. Tech. Phys.*, 19:351.

Taylor, M. J. and Clark, S. (1996). High resolution CCD and video imaging of sprites and elves in the N_2 first positive band emission. *Eos Trans. AGU - Fall Meet. Suppl.*, 77(46):F60.

Uman, M. A. (2001). *The Lightning Discharge*. Dover Publications, New York.

Vallance-Jones, A. V. (1974). *Aurora*. D. Reidel Publishing Co.

van Veldhuizen, E. M., editor (2000). *Electrical discharges for environmental purposes: Fundamentals and applications*. Nova Science, New York.

van Veldhuizen, E. M. and Rutgers, W. R. (2002). Pulsed positive corona streamer propagation and branching. *J. Phys. D: Appl. Phys.*, 35:2169–2179.

Veronis, G., Pasko, V. P., and Inan, U. S. (1999). Characteristics of mesospheric optical emissions produced by lightning discharges. *J. Geophys. Res.*, 104:12,645–12,656.

Vitello, P. A., Penetrante, B. M., and Bardsley, J. N. (1993). Multidimensional modeling of the dynamic morphology of streamer coronas. In *Non-Thermal Plasma Techniques for Pollution Control*, volume G34, part A of *NATO ASI Ser.*, pages 249–271. Springer-Verlag, New York.

Vitello, P. A., Penetrante, B. M., and Bardsley, J. N. (1994). Simulation of negative-streamer dynamics in nitrogen. *Phys. Rev. E*, 49:5574–5598.

Wescott, E. M., Sentman, D., Osborne, D., Hampton, D., and Heavner, M. (1995). Preliminary results from the Sprites94 aircraft campaign: 2. Blue jets. *Geophys. Res. Lett.*, 22:1209–1212.

Wescott, E. M., Sentman, D. D., Heavner, M. J., Hampton, D. L., Osborne, D. L., and Vaughan Jr., O. H. (1996). Blue starters: Brief upward discharges from an intense Arkansas thunderstorm. *Geophys. Res. Lett.*, 23:2153–2156.

Wescott, E. M., Sentman, D. D., Heavner, M. J., Hampton, D. L., and Vaughan Jr., O. H. (1998). Blue jets: their relationship to lightning and very large hailfall, and their physical mechanisms for their production. *J. Atmos. Sol.-Terr. Phys.*, 60:713–724.

Wescott, E. M., Sentman, D. D., Stenbaek-Nielsen, H. C., Huet, P., Heavner, M. J., and Moudry, D. R. (2001). New evidence for the brightness and ionization of blue starters and blue jets. *J. Geophys. Res.*, 106:21549–21554.

Wilson, C. T. R. (1925). The electric field of a thundercloud and some of its effects. *Proc. Phys. Soc. London*, 37(32D–37D).

Winn, W. P., Schwede, G. W., and Moore, C. B. (1974). Measurements of electric fields in thunderclouds. *J. Geophys. Res.*, 79:1761–1767.

Yair, Y., Israelevich, P., Devir, A. D., Moalem, M., Price, C., Joseph, J. H., Levin, Z., Ziv, B., Sternlieb, A., and Teller, A. (2004). New observations of sprites from the space shuttle. *J. Geophys. Res.*, 109:doi:10.1029/2003JD004497.

Yair, Y., Price, C., Levin, Z., Joseph, J., Israelevitch, P., Devir, A., Moalem, M., Ziv, B., and Asfur, M. (2003). Sprite observations from the space shuttle during the Mediterranean Israeli dust experiment (MEIDEX). *J. Atmos. Sol.-Terr. Phys.*, 65(5):635–642,doi:10.1016/S1364–6826(02)00332–2.

Yi, W. J. and Williams, P. F. (2002). Experimental study of streamer in pure N_2 and N_2/O_2 mixtures and a $\approx$13 cm gap. *J. Phys. D: Appl. Phys.*, 35:205–218.

Yukhimuk, V., Roussel-Dupré, R. A., and Symbalisty, E. M. D. (1999). On the temporal evolution of red sprites: Runaway theory versus data. *Geophys. Res. Lett.*, 26:679–682.

Yukhimuk, V., Roussel-Dupré, R. A., Symbalisty, E. M. D., and Taranenko, Y. (1998a). Optical characteristics of blue jets produced by runaway air breakdown, simulation results. *Geophys. Res. Lett.*, 25:3289–3292.

Yukhimuk, V., Roussel-Dupré, R. A., Symbalisty, E. M. D., and Taranenko, Y. (1998b). Optical characteristics of red sprites produced by runaway air breakdown. *J. Geophys. Res.*, 103:11473–11482.

Zabotin, N. A. and Wright, J. W. (2001). Role of meteoric dust in sprite formation. *Geophys. Res. Lett.*, 28(13):doi:10.1029/2000GL012699.

Zheleznyak, M. B., Mnatsakanyan, A. Kh., and Sizykh, S. V. (1982). Photoionization of nitrogen and oxygen mixtures by radiation from a gas discharge. *High Temp.*, 20:357–362.